LOST FOAM CASTING OF LM6-Al-Si CAST ALLOY

MOHAMMED.BSHER.A.ASMAEL

A project report submitted in the fulfillment
of the requirements for the award of the degree of Master of Engineering
(Mechanical - Advanced Manufacturing Technology)

Faculty of Mechanical Engineering
Universiti Teknologi Malaysia

MAY 2009

To My Beloved Mother, Father, Brothers and Sisters

.

ACKNOWLEDGMENTS

In the name of Allah, Most Gracious, and Most Merciful I would like to thank the many people who have made my master project possible. In particular I wish to express my sincere appreciation to my supervisors Associate Professor Dr Mohd Hasbullah Idris and Associate Professor Dr. Ali Ourdjini, for their encouragement, guidance, critics and friendship.

I would never have been able to make accomplishment without the loving support of my family.

I would also like to thank all technicians and fellow researchers in the casting and materials science laboratories especially Mr. Wan.

I would like to thank my colleagues especially Mr. Kajed and Alsalhin G.

My sincere appreciation extends to all my friends and others who have provided assistance. Their views and tips were useful indeed. Unfortunately, it is not possible to list all of them in this limited space. I am grateful having all of you beside me. Thank you very much.

ABSTRACT

In the present research, experimental investigation of an investigation of lost foam casting of LM6-Al-Si cast alloy has been conducted. The investigation has as main objectives to investigate the effect of pouring temperature and melt treatment by addition of grain refiner on the microstructure and mechanical properties of lost foam castings of the LA-Si alloy. Castings in the shape of step-like with five sections were produced mainly using a foam density of 20 kg/m³ and pouring was made at five different temperatures of 700,720,740,760,780^{o}C with and without the presence of AlTiB grain refiner in the melt. The different pouring temperatures would permit obtaining castings at different cooling rates. The results obtained showed that pouring temperature has a significant influence on the quality as well as microstructure of lost foam casting of LM6-Al-Si alloy. Lower pouring temperature provides finer microstructure and high hardness and that faster cooling rate produced either by lower pouring temperature or thinner section would results in enhanced hardness. However, the addition of AlTiB as grain refiner did not affect the castings produced significantly whether in terms casting quality or microstructure.

ABSTRAK

Dalam kajian menunjukkan, siasatan percubaan satu siasatan tuangan busa hilang bagi kas LM6 A1 Si aloi telah dijalankan. siasatan telah sebagai objektif-objektif utama untuk menyiasat kesan menuang suhu ans cair rawatan oleh tambahan mendapat penghalus pada mikrostruktur dan ciri-ciri mekanikal acuan-acuan busa hilang aloi LA Si aloi. acuan-acuan dalam bentuk langkah seperti dengan lima bahagian-bahagian telah dihasilkan terutamanya menggunakan satu ketumpatan busa 20kg/m³ dan menuang adalah dibuat pada lima suhu yang berbeza 700,720,740,760,780^{o}C dengan dan tanpa kehadiran bagi A1TiB penghalus bijian dalam cair. berbeza menuang suhu akan membenarkan mendapatkan pemilihan pelakon pada kadar-kadar pendinginan berbeza. keputusan itu memperolehi menunjukkan yang menuang suhu mempunyai satu pengaruh penting pada kualiti serta mikrostruktur tuangan busa hilang LM6-Al-Si aloi. mengurangkan menuang suhu menyediakan mikrostruktur yang lebih baik kekerasan tinggi dan yang cepat kadar penyejukan menghasilkan sama ada dengan mengurangkan menuang suhu atau seksyen lebih kurus akan mengakibatkan kekerasan ditingkatkan. bagaimanapun,tambahan bagi A1TiB sebagai penghalus bijian melakukan tidaklah menjejaskan acuan-acuan itu menghasilkan nyata sekali sama ada dalam bertempoh membuang kualiti atau mikrostruktur

TABLE OF CONTENTS

CHAPTER	TITLE	PAGE
	DECLARATION	ii
	DEDICATION	iii
	ACKNOWLEDGEMENTS	iv
	ABSTRACT	vi
	ABSTRAK	vii
	TABLE OF CONTENTS	viii
	LIST OF TABLES	xii
	LIST OF FIGURES	xiii
1	**INTRODUCTION**	
	1.1 Background	1
	1.2 Problem Statement	1
	1.3 Objective of the Project	2
	1.4 Scope of the Project	3
2	**LITERATURE REVIEW**	4
	2.1 Aluminium and its alloys	4
	2.1.1 Classification of Aluminium Alloys	5
	2.1.1.1 Casting Alloys	6

2.1.1.2 Wrought Alloys 7
2.1.2 Applications of Aluminium Alloys 8
2.2 Al-Si Casting alloys 8
2.2.1 Solidification of Al-Si Alloys 9
2.2.2 Cooling curve 11
2.2.3 Aluminum – silicon – LM6 alloys 12
2.2.4 Hypereutectic Al-Si Alloys 15
2.2.5 Grain Refinement of Hypereutectic 16
2.2.6 Modification of Al-Si Alloys 18
2.2.7 Chemical modification 20
2.3 Nucleation 22
2.3.1 Homogeneous nucleation 23
2.3.2 Heterogeneous nucleation 23
2.4 Growth 24
2.4.1 Solidification of dendrite 25
2.4.2 Shrinkage solidification 27
2.4.3 Chvorino’s Rule 27
2.6 Lost Foam Casting (LFC) 28
2.6.1 Preparation of bead of polystyrene 29
2.6.2 Pattern Making 30
2.6.3 Coating 30
2.6.4 Sand filling and vibration , compaction 31
2.6.5 Lost Foam Filling Mechanism 32
2.7 Parameters affecting on LFC 33
2.7.1 Degree of vacuum 33
2.7.2 Permeability pattern coatings 34
2.7.3 Pressure 35
2.7.4 Pouring temperature 35

3	**RESEARCH METHODOLOGY**		36
	3.1 Introduction		36
		3.1.1 Pattern making	38
		3.1.2 Pattern coating and dry	39
		3.1.3 Sand filling and vibration	41
		3.1.4 Temperature measurement	43
		3.1.5 Melting procedure and casting	44
	3.2 Analysis		46
		3.2.1 Casting analysis	46
		3.2.2 Microstructure Analysis	47
		3.2.2.1 Simple preparation	47
		3.2.2.2 Image Analysis (Eutectic Spacing Measurements)	48
		3.2.3 Mechanical properties	49
		3.2.3.1 Tensile test	49
		3.2.3.2 Vickers Hardness	51
4	**RESULTS AND DISCUSSION**		52
	4.1 Introduction		52
	4.2 Casting analysis		52
	4.3 Microstructure		55
	4.4 Mechanical properties		63
		4.4.1 Hardness test	63
		4.4.2 Tensile test	64
5	**CONCLUSIONS AND FUTURE WORK**		69
	5.1 Conclusions		69
	5.2 Recommendations for future work		70
	REFERENCES		71

LIST OF TABLES

TABLE NO	TITLE	PAGE
2.1	The general characteristics of aluminium	5
2.2	Cast aluminum alloy groups	6
2.2	Wrought aluminum alloy groups	7
2.3	Applications of cast aluminium	7
2.4	Some properties of possible modifier	19
3/1	Chemical composition of LM6 Alloy	41
3.2	TENSILE STRENGTH & HARDNESS	47

LIST OF FIGURES

FIGURE NO	TITLE	PAGE
2.1	Phase diagram of Al-Si alloy	9
2.2	Types of microstructures that may form during Solidification of a casting	10
2.3	cooling curve for a hypo hypereutectic alloy	11
2.4	Aluminum – silicon phase diagram and microstructures	12
2.5	Cooling curve of a cooled metal.	13
2.6	Methodology for measurement of DAS	16
2.7	Optical micrographs showing the various phases observed	17
2.8	Microstructure of a (a) unmodified and (b) modifi Hypoeutectic Al–Si alloy	18
2.9	The variation of free energy with radius of nucleus	21
2.10	Transition of growth morphology	23
2.11	Schematic illustration of three basic types of cast structures	24
2.12	Lost foam steps	27
2.13	Lost foam process	29
2.14	Schematic of molten metal front in LFC	30
2.15	IShikawa cause effect diagram of LFC process	31
3.1	experimental steps	35
3.2	Pattern dimensions	36
3.3	Sections of the pattern	37

3.4	coating mixer	38
3.5	flow cup	38
3.6	patterns after coating	38
3.7	Flask position	39
3.8	sand filling and vibration	41
3.9	Shaft used to mixed the TiB	42
3.10	induction furnace	43
3.11	Pouring of castings	43
3.12	Sample preparation for microstructure analysis	44
3.13	Method showing the measurement of eutectic spacing	45
3.14	Tensile specimens test dimensions	46
4.1	Castings using 16, 20 and 32 foam density	51
4.2	Effect of pouring temperature on microstructure on untreated LM6	52
4.3	Effect of pouring temperature on microstructure on TiB-treated LM6 alloy	53
4.4	Effect of pouring temperature on microstructure on untreated and TiB-treated LM6 alloy cast at 740C° for 3, 12 and 24 mm sections	54
4.5	Effect of pouring temperature on eutectic spacing in 3mm thickness (fast cooling rate) for unmodified casting	55
4.6	Effect of pouring temperature on eutectic spacing in 3mm thickness (fast cooling rate) for grain refined casting	56
4.7	Effect of pouring temperature on eutectic spacing in 12mm thickness for unmodified casting	56
4.8	Effect of pouring temperature on eutectic spacing in 12mm thickness for grain refined casting	57
4.9	Effect of pouring temperature on eutectic spacing in 24mm thickness (lower cooling rate) for unmodified casting	57
4.10	Effect of pouring temperature on eutectic spacing in 24mm thickness (lower cooling rate) for grain refined casting	58

4.11	Effect of pouring temperature, section thickness and grain refiner on eutectic spacing	59
4.12	Effect of pouring temperature on hardness	60
4.13	Some of the defects observed in the castings (gas porosity, penetrate of coating into the metal and shrinkage)	61
4.14	Effect of pouring temperature on experimental tensile strength	62
4.15	Comparison of experimental and theoretical tensile strength as function of pouring temperature	63
4.16	Effect of pouring temperature on theoretical tensile strength	63

CHAPTER 1

INTRODUCTION

1-1 Background

Aluminum alloy castings are widely used in the automobile and aerospace industries, and are replacing heavier forged steel or cast iron for the lighter and more fuel efficient automobiles. Producing defect free Al castings becomes more important. Aluminum alloys are used extensively due to their high strength to weight ratio, good Machinability, corrosion resistance, optimum surface finish, and high electrical and thermal conductivity.[1]

Lost foam casting is a full mould process, which uses a polystyrene foam pattern in unbonded sand. The foam pattern is prepared by injecting expandable polystyrene beads under the combined action of steam and pressure. Then, the pattern assembly is coated with refractory slurry and dried. The coated pattern assembly is set in a steel flask, which is then filled with unbounded sand. The flask is vibrated to compact the sand. Finally, molten metal is poured directly into the coated pattern assembly. The polymer pattern undergoes thermal degradation and is replaced by the molten metal [2].

LFC has a number of advantages as it allows the caster to design complex shapes without cores and parting lines, enables lighter castings with minimum wall thickness, reduces secondary machining requirements and provides close dimensional tolerance and good surface finish. The use of unbounded sand provides a further advantage. The disposal of sand in conventional sand casting is an environmental issue involving high cost; however in LFC sand can be reused easily and the cost for sand reclamation and sand disposal is not high. There is less room for errors in LFC [3]. In fact, a scrapped casting means replacing not only the mould but the pattern as well. The pouring is hazardous, pattern coating and drying are time consuming and pattern handling requires great care.

1.2 Problem statement

The properties of Al- Si alloys are controlled by the phases that constitute the alloy (Al and Si). In particular, many of the considerations arise due to processing.The pouring temperature for instance directly affects the nucleation and growth of primary phases (Al or Si) in Al–Si alloys. Pouring temperature determines the cooling rate and nucleation controls the size of grains formed while growth determines the grain morphology and the distribution of alloying elements within the matrix. This is the reason why pouring temperature is recommended by many researchers, who studied microstructure and mechanical properties this material.

1.3 Objectives of Study

Investigate the effect of pouring temperature (cooling rate) and melt treatment (addition of grain refiner) on microstructure and mechanical properties of lost foam casting of LM6 Al-Si alloy

1.4 Scope of Study

1- LFC casting of Al-Si (LM6) alloy
2- Microstructure analysis with focus on grain size (eutectic silicon spacing) and porosity
3- Evaluation of the mechanical properties: hardness and tensile properties

CHAPTER 2

LITERATURE REVIEW

2.1 Aluminium and Its Alloys

Aluminum is the third most abundant element in the Earth's crust and constitutes 7.3% by mass. In nature, however it only exists in very stable combinations with other materials (particularly as silicates and oxides) and it was not until 1808 that its existence was first established.

The metal originally obtained its name from the Latin word for alum, alumen. The name alumina was proposed by L.B.G de Moreveau, in 1761 for the base in alum, which was positively shown in 1787 to be the oxide of a yet to be discovered metal. Finally, in 1807, Sir Humphrey Davy proposed that of aluminum so to agree with the “ium” spelling that end most of the elements

Table2.1: The general characteristics of aluminium.

Characteristics of aluminium	
Symbol	Al
atomic number	13
atomic weight	26.98
Density	2698 kg
melting point	660.37
boiling point	2467 °c
electrical resistively	26.548 · 10-3 μ · m (to 25°C)
Thermal Conductivity	237 W/m · K (to 27 °C)

2.1.1 Classification of Aluminium Alloys

Aside from steel and cast iron, aluminium is one of the most widely used metals owing to its characteristics of lightweight, good thermal and electrical conductivities. Despite these characteristics, however, pure aluminium is rarely used because it lacks strength. Thus, in industrial applications, most aluminium is used in the form of alloys.

There are a number of elements that are added to aluminium in order to produce alloys with increased strength and improved foundry or working properties. In addition to alloying aluminum with other elements, the mechanical properties can also be enhanced by heat treatment. Generally, aluminium alloys can be classified into two main categories: cast alloys and wrought alloys.

2.1.1.1 Casting Alloys

These alloys suffer from higher shrinkage (up to 7%) which occurs during cooling or solidification. Higher mechanical properties in these alloys can be achieved by controlling the level of impurities, grain size, and solidification parameters such as the cooling rate.

A system of four-digit numerical designation is used to identify aluminium and aluminium alloys in the form of castings and foundry ingots. The first digit indicates the alloy group as shown in Table 2.2. The second and third digits identify the aluminium alloy or indicate the minimum aluminium percentage. The last digit, which is to the right of the decimal point, indicates the product form: XXX.0 indicates castings, and XXX.1 and XXX.2 indicate ingots.

Aluminum 99% minimum and greater	1xx.x
Aluminium alloy with major alloying elements as copper	2xx.x
Manganese	3xx.x
Silicon	4xx.x
Magnesium	5xx.x
Magnesium	6xx.x
Zinc	7xx.x
Other element	8xx.x
Unused	9xx.x

Table 2.2: Cast aluminum alloy groups

2.1.1.2 Wrought Alloys

These are alloys are shaped using certain working processes and are used as rolled plates, sheet metal, foil, extrusion tubes, rods, bars and wire. Wrought alloys are also designated by a four digit system. Both wrought and cast aluminium alloys are divided into alloys which can be heat treated (in order to increase the mechanical properties) and alloys which cannot be heat treated.

Aluminum 99% minimum and greater	1xxx
Aluminum alloys with major alloying elements copper	2xxx
Silicon, with added copper and / or magnesium	3xxx
Silicon	4xxx
Magnesium	5xxx
Unused series	6xxx
Zinc	7xxx
Tin	8xxx
Other element	9xxx

Table2.2: Wrought aluminum alloy groups

2.1.2 Applications of Aluminium Alloys

Table 2.3: some typical applications of cast aluminium alloys include the following:

Alloy Type	Typical Applications
319.0	Manifolds, cylinder heads, blocks, internal engine parts.
332.0	Pistons.
356.0	Cylinder heads manifolds.
A356.0	Wheels.
A380.0	Blocks, transmission housings/parts, fuel metering devices.
383.0	Brackets, housings, internal engine parts, steering gears.
B390.0	High-wear applications such as ring gears & internal transmission Parts.

2.2 Al-Si Casting Alloys

Over the last 50 years, there has been a growing trend towards lightweight materials because of environmental concerns and for producing components and structures at low cost with increased performance. Al-Si casting alloys are the most widely used alloys due to the following characteristics [3]:

• Low density

• Excellent fluidity (due to addition of silicon)

• Good weld ability

• High corrosion resistance

• Low coefficient of thermal expansion (CTE

2.2.1 Solidification of Al-Si Alloys:

Al-Si alloys differ from the "standard" phase diagram in that aluminium has zero solid solubility in silicon at any temperature. This means that there is no β phase and so this phase is "replaced" by pure silicon. So, for Al-Si alloys, the eutectic composition is a structure of α + Si rather than α +β. Figure 2.1 shows the Al-Si phase diagram.

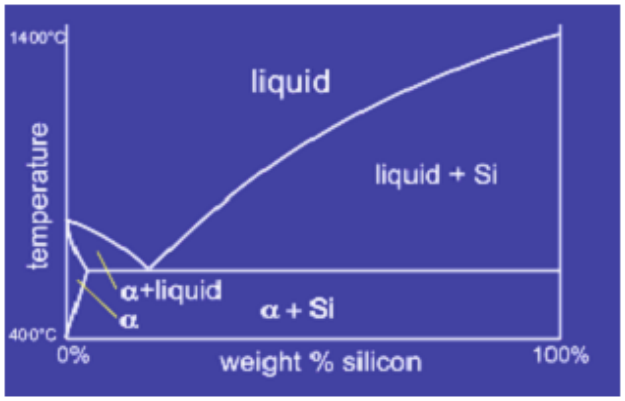

Figure 2.1: Phase diagram of Al-Si alloy

The solidification of Al-Si alloys is an important aspect because it controls the final microstructure which in turn controls the mechanical properties. Therefore, it is necessary to understand the basic principle of solidification and how the microstructure form. In general, solidification of an alloy occurs in two stages:

During the first step, the aluminium dendrites nucleate and grow between the liquid and eutectic temperature also known as the mushy zone. When the Mushy zone width increases there is a higher dendrite volume fraction, which reduces the final volume fraction of the eutectic liquid. As result the shrinkage pressure increases. The

pressure due to interna1 gas and shrinkage pressures are not large enough to overcome the surface tension at this stage and as a result very few gas pores are expected to grow.

Solidification occurs during the eutectic plateau developing at 577 ^{o}C. The eutectic cells begin to grow containing eutectic Al, Si, FeSi and Mg2Si [20]. Typically, the eutectic liquid interface is irregular and when new pores develop during the eutectic region, they follow the contour of the Al dendrites and irregular eutectic cells creating inter-dendritic porosity. Small eutectic cells promote the formation of clusters of inter-dendritic pores. As solidification a proceeds, the inter-dendritic flow is further reduced thereby increasing the shrinkage pressure and could result in shrinkage porosity. The interna1 gas pressure is maximum at this stage and if there is sufficient hydrogen in the inter-dendritic pockets, small gas pores will develop.

There are two types of grain structures that may be formed upon solidification of a metal alloy: columnar and equiaxed grains. Equiaxed grains form as a result of equal growth in all directions of the crystal (prevalent in grain refined alloy due to the presence of large number of nucleation sites) while columnar grains are present as thin, long structures which grow under a temperature gradient during slow solidification. These columnar grains grow in a direction normal to the mould wall and in a direction opposite the heat flow

The preferred structure of a casting is one that has small equiaxed grains (Figure 2.2), since this type of structure improves feeding, resistance to hot tearing and enhances the mechanical properties. Improvements in the mechanical properties are the result of sound casting that can be produced during casting. Producing a structure with equiaxed grains can be achieved through control of the solidification conditions or by the use of inoculants or grain refiners.

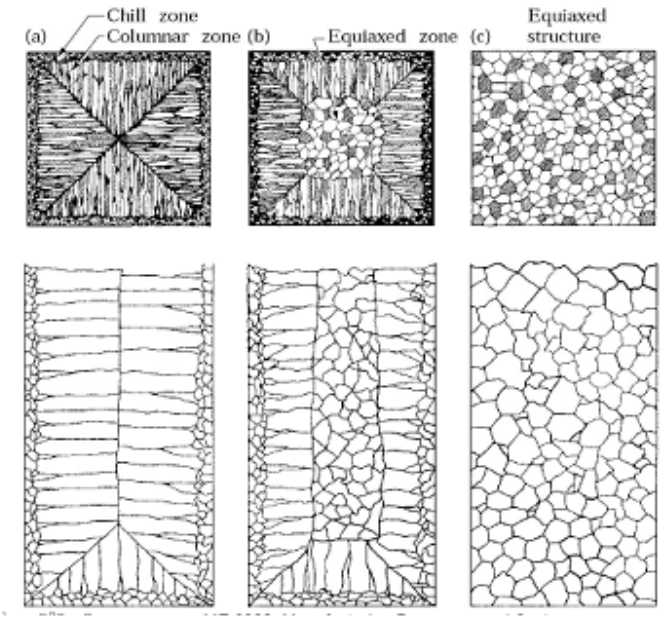

Figure 2.2: Types of microstructures that may form during solidification of a casting [4].

2.2.2 Cooling curve

The cooling curve is the relationship between the time and temperature relationship obtained during the solidification of a metal or alloy. A typical cooling curve for a hypereutectic alloy is shown in Figure 2.3. The eutectic solidification starts at point (2). The release of the latent heat occurs at this point, and the cooling continues at a constant temperature (eutectic plateau). Finally the solidification is completed at point (3).

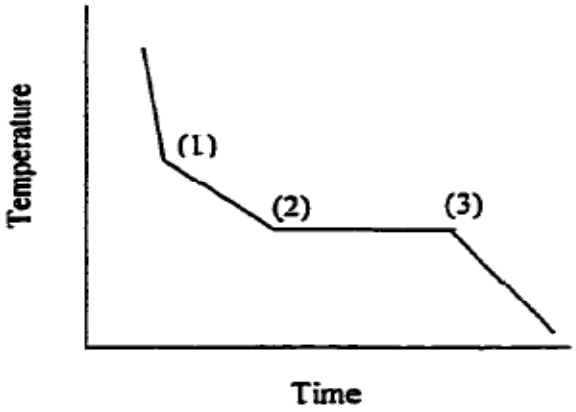

Figure 2.3: Idealized example of simple cooling curve for a hypo hypereutectic alloy,

2.2.3 Aluminum – silicon – LM6 alloys

Aluminum–silicon alloys are widely used for shape casting due to their high fluidity, ease of casting, low density and controllable mechanical properties. Commercial Al-Si alloys are available in alloys with silicon additions of up to 11 %(hypoeutectic), 11 to 13% (eutectic) or over 13% (hypereutectic). Various other elements such as Fe, Cu, Mg, Ni, and Zn are added to achieve the optimum casting or mechanical properties.

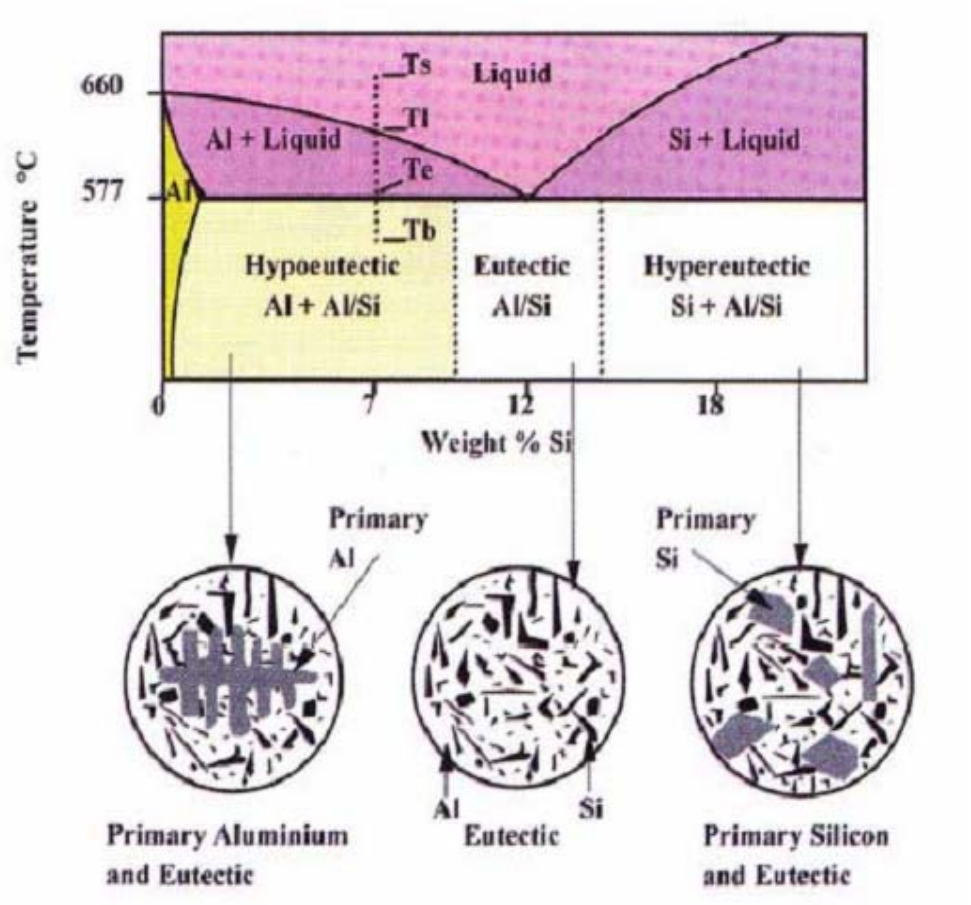

Figure 2.4: Aluminum – silicon phase diagram and microstructures [2].

According to Figure 2.4, upon solidification of aluminum–silicon alloys of composition generally less than 12% silicon (hypoeutectic) the first phase to form is aluminum. Considering an alloy containing 7% silicon on cooling form the liquid phase (Ts) the aluminum forms as small dendrites when the solidification temperature (Tl) is reached. The temperature difference Ts-Tl is the melt "superheat" or under cooling, which represents the driving force for solidification. Solidification does not occur at a single temperature but rather over a temperature range and will be completed at the eutectic temperature (Te). The exception is the case of alloys of eutectic composition (~12% Si) where solidification occurs at the eutectic temperature. As the temperature

falls below the liquids point (TI), aluminum dendrites grow and more are nucleated until the eutectic temperature is reached. The dendrites formed are seen as the aluminum grains in the final microstructure. At the eutectic temperature all of the remaining liquid will freeze as aluminum–silicon eutectic in simple binary alloys. However, various other intermetallic phases such as CuAl2, Mg2Si will form at lower temperatures in commercial alloys depending on the actual alloy composition.

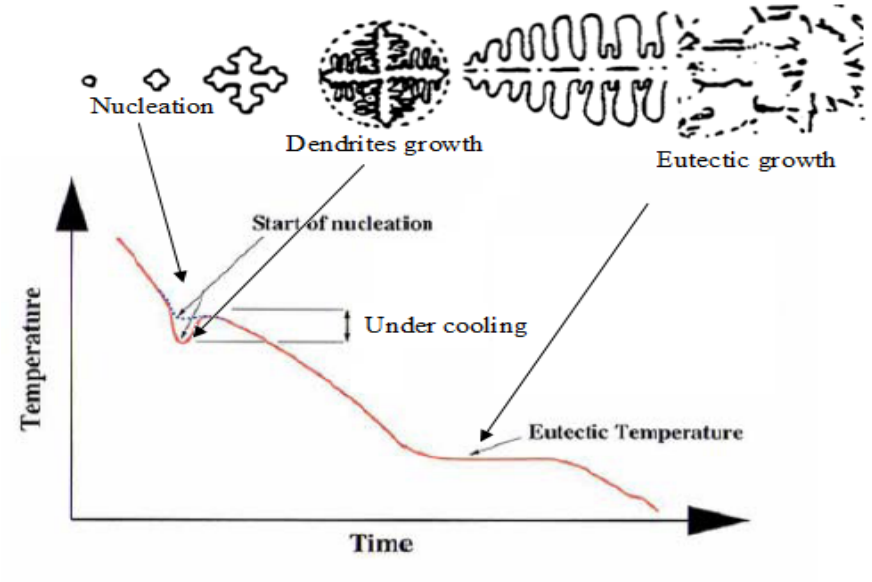

Figure 2.5: Cooling curve of a cooled metal.

Because solidification liberates heat, we would expect to see a plateau in the melt temperature on a thermal analysis trace when it occurs. In practice, cooling below the equilibrium point is required in order to nucleate the first dendrites. As those dendrites grow, heat is liberated and the temperature will rise (Figure 2.5). The temperature drop required "undercooling", and is a measure of the difficulty in nucleation of the first aluminum dendrites. Grain refined alloys have very low undercooling compared to non-grain refined alloys because the action of the refiner is to aid nucleation. Following the temperature rise it will fall again as heat is extracted, until the eutectic temperature is reached when it stabilizes while solidification of aluminum-silicon is completed. Further

arrests in the temperature trace may also be seen as intermetallic phases during cooling. The structure of the alloy will thus be comprised of a mixture of dendritic grains surrounded by aluminium-silicon eutectic with isolated pockets of intermetallics and shrinkage porosity.

2.2.4 Hypereutectic Al-Si Alloys

Hypereutectic Al-Si casting alloys (> 13%Si) are widely used in the automotive industry. Components such as engine blocks, pistons, cylinders, and pump components are made from this category of alloys. The hypereutectic Al-Si alloys contain hard primary particles of non-metallic silicon embedded in an Al-Si eutectic matrix. Hypereutectic alloys possess outstanding wear resistance and good elevated temperature strength, lower thermal expansion coefficient (CTE), very good casting characteristics and excellent strength to weight ratio. One of the most widely used hypereutectic Al-Si alloys is the 390 alloy, which possesses excellent fluidity and has good resistance to hot cracking during casting.

The impurities and alloying elements can go into the solid solution in the matrix or produce an intermetallic, compound during the solidification process. In hypoeutectic alloys, the following phenomena are known to occur.

- Formation of dendrite network of a aluminum.
- An aluminum-silicon eutectic reaction
- Precipitation of secondary eutectic phases such as Mg2Si

The existence of these structures reflects the complexity of the solidification process of a casting, as they are often due to melt treatment or casting conditions.

Primary silicon in hypereutectic Al-Si alloys may appear in several different morphologies, and it is not uncommon to find many of these in the same casting. The morphology of silicon in hypereutectic alloys is highly dependent on the solidification parameters such as: cooling rate, temperature gradient in the liquid and presence of inoculants. Hypereutectic Al-Si alloys also suffer from macro-segregation, particularly under slow solidifications conditions as in sand casting for example. Additions of phosphorous as well as strontium to these alloys may reduce silicon segregation in casting by providing longer flotation time or short primary solidification temperature range. Cooling the casting at higher solidification rate in excess of 15° C/S was found to reduce segregation of primary silicon.

2.2.4 Grain Refinement of hypereutectic Al-Si Alloys

Usually the aluminum alloys, form coarse, equated and columnar crystals (grains) during solidification. The degree of coarseness or the length of columnar crystals depends on the:

- solidification
- casting parameters including :

1- pouring temperature,
2- liquid thermal gradient in the mould
3- Alloying elements. It should be noted that all the common alloying elements added to aluminium reduce the grain size somewhat. Generally, the more soluble are the elements, the greater the refinement.

Close control of the as-cast structure is required in the production of quality aluminium products. The fine-grained of structure provides a number of technical and economical advantages, including improved mechanical properties, increased casting speed, reduced cracking and better post solidification deformation characteristics (It

should be pointed out that the properties in alloys which contain a large eutectic fraction, such as Al-Si alloys, are dependent on both the grain size and eutectic structure) [7]

There are three principal methods for achieving grain refinement in Al alloys:

a) Fast cooling during solidification (chill grain refinement)

A fine grain structure is formed by varying the solidification conditions such as cooling rate and temperature gradient in the casting. This is due to shortening of grain growth during the solidification process.

b) Agitation of the melt as for instance during semi-solid metal processing.

Grain refinement is achieved by mechanical or electromagnetic agitation, forced convection, by breaking up the dendrites in the semi-solid state. The fragmented parts are transported into the bulk and become effective nucleates. This is the type of refinement mechanism when stirring is applied during the formation of the semi-solid structure. By far, the most successful method to control the grain size is to introduce into the melt particles that nucleate new crystals during solidification.

c) Addition of a grain refiner to the melt.

The fragmented parts are transported into the bulk and become effective nucleates. This is the type of refinement mechanism when stirring is applied during the formation of the semi-solid structure. By far, the most successful method to control the grain size is to introduce into the melt particles that nucleate new crystals during solidification. Each grain contains a family of aluminium dendrites originated from the same nucleus. Dendritic arm spacing (DAS) as in Figure 2.6 is determined by the cooling rate through the mushy zone, with slower cooling resulting in larger values of DAS. The grain size in aluminium foundry alloys varies between 1-10 mm, DAS values vary from 10 to 150 um

and the eutectic silicon may be found in plates up to 2 mm in length or spheres of less than 1 um in diameter [8]

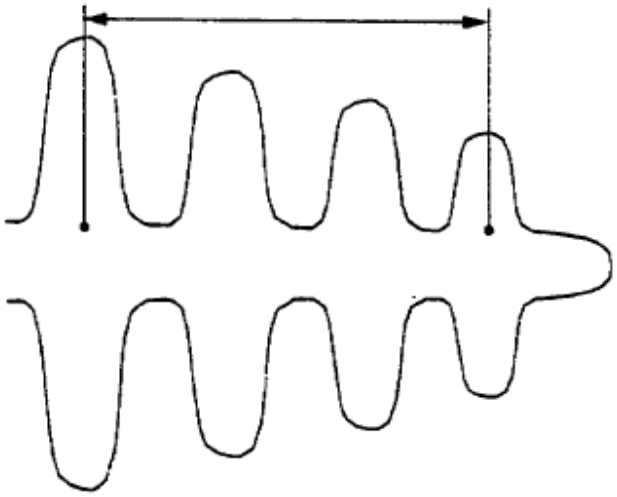

$$DAS = at^n$$

Figure 2.6: Methodology for measurement of DAS

2.2.5 Modification of Al-Si Alloys

Modification is a process that changes the microstructure of cast alloys either through quenching or by adding some alkaline elements. In addition, modification has become a common and sometimes an essential foundry practice when it comes to casting the aluminium-silicon alloys. The importance of modification in a casting is to achieve a different microstructure that can yield better mechanical properties and characteristics. Basically, modification can be divided into impurity modification and quench modification. Modification through the additions of a small amount of modifiers is termed impurity modification while the latter is due to rapid solidification rate. Although there are many elements, which are found to have modification ability, only sodium and

strontium appear to be stronger modifiers at low concentration and now they are widely used for commercial applications. In hypoeutectic Al-Si alloys, silicon is present as a constituent of the eutectic phase, so sodium and strontium transform the flake eutectic silicon into fibrous form, hence increasing the ultimate tensile strength, ductility, hardness and machinability. Modification is affected by several variables and reversion of the modified structure back to the unmodified state is possible when there is higher silicon content, higher temperature and longer holding times.

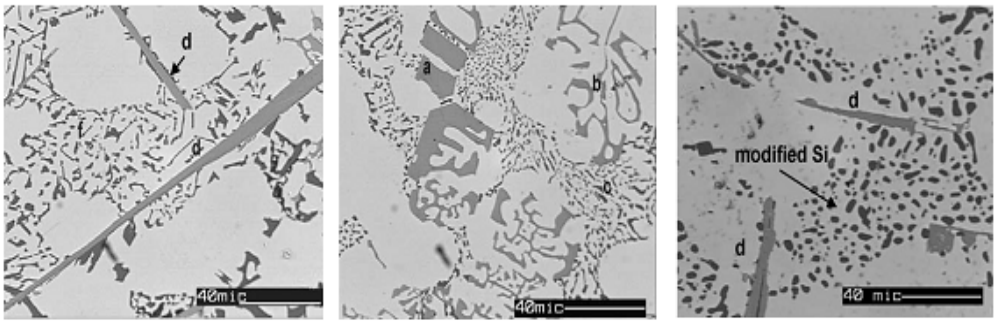

Figure 2.7: Optical micrographs showing the various phases observed.

Solidification is therefore suppressed to lower temperatures where the nucleation rate is large. This leads to a remarkable refinement of microstructure. Figure 2.7 and Figure 2.8 show the silicon morphology of an unmodified and modified alloy.

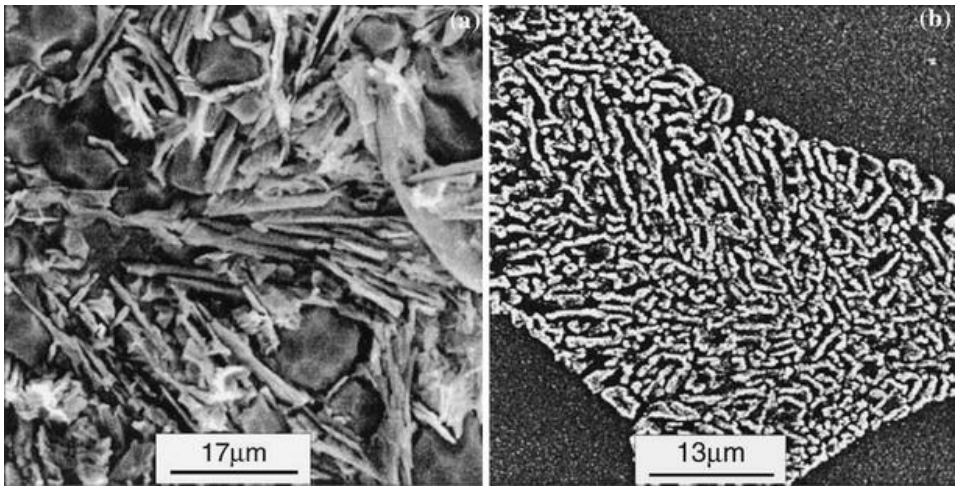

Figure.2.8: Microstructure of a (a) unmodified and (b) modified Hypoeutectic Al–Si alloy

In hypereutectic alloys, however, silicon is present both as a eutectic constituent and as primary phase. Thus modification induces another transition which is a transition of the primary silicon involving three apparent possibilities irregular to dendritic, irregular to spheroidal, and dendritic to spheroidal [5].

2.2.6 Chemical modification

Certain elements, such as calcium, sodium, strontium, and antimony, which are added to hypoeutectic Al-Si alloys results in a finer lamellar or fibrous eutectic network. While a number of IA and IIA elements and several lanthanides produce a modified silicon eutectic, only Sr, Na, and Sb have found extensive commercial application during the last three decades. The amount of each element required depends on the alloy composition, impurities in the melt, and freezing rate. A study on this ratio for elements that are known to modify to some extent, indicates they all have a radius ratio in the

vicinity of the ideal value; some are presented in Table 2.5. It is noticeable that the size of sodium atoms is closer to the ideal

Element	Atomic radius (A°)	r/rsi	Melting point	Vapor pressure (atm)	AG oxide (kJmol"1)	K"-oxidation
Ba	2.18	1.85	725	$5 * 10^{-3}$	482	20
Sr	2.16	1.84	769	$1 * 10^{-3}$	480	15
Eu	2.02	1.72	822	$1.8 * 10^{-4}$	500	-
Ca	1.97	1.68	839	$2.6 * 10^{-4}$	509	400
Yb	1.93	1.65	824	$5.6 * 10^{-3}$	500	1500
La	1.87	1.59	926	10^{-6}	487	-
Na	1.86	1.58	98	0.2	367	$2.7 * 10^{-5}$
Ce	1.83	1.56	798	10^{-16}	497	-

Table 2.4: Some properties of possible modifier

Some other factors that are significant in determining the ability of any element to modify the silicon are listed in Table 2.5. The melting point is important because elements that melt at lower temperatures will presumably dissolve more readily in Al-Si melts that are typically held at higher temperatures. Thus, sodium dissolves easily but strontium has some difficulty and other elements on the list are even more difficult to dissolve. The vapour pressure is of significance since elements with high vapour pressure tend to boil off the melt. The well known fading effect of Na is due to its high vapour pressure while Sr and all of the remaining elements are much more stable in the melt. In addition to vaporization, effective modifiers may be lost through K-oxidation. The values in Table 2.5 are the equilibrium constants for the following reaction:

$$X\ Al_2O_3 + Y\ Modifier \text{ -» } 2x\ Al + 3\ ModifierXOY$$

Large values of this parameter are indicative of a high tendency to oxidation. Therefore, while sodium vaporizes, it does not oxidize. Strontium, on the other hand is lost by slow oxidation and the oxidation of Ca and Y is very severe [6].

2.3 Nucleation

It is controls the structure and hence the properties of castings this is why the nucleation is important. The metal liquid cools under the freezing point also the thermal agitation decreases. The small groups of some locations which move to crystalline arrangement and form clusters then form nuclei. For small nuclei, the net energy to form this new phase is reduced in proportion to its volume (V) and the free energy per unit volume (ΔGv); however, it increases in proportion to the surface area and solid- liquid surface energy (y). For spherically-shaped nuclei, the free energy is calculated thus, Porter [7]

$$\Delta G = 4\pi r^2 y - 4/3\pi r^3\ \Delta Gv \ldots\ldots\ldots\ldots\ldots\ldots\ldots\ldots\ldots\ldots (1)$$

Therefore the critical or minimum radius of nuclei (**r'**) is obtained by differentiating Equation (1)

$$\partial(\Delta G)/\partial r = 0 \Longrightarrow \pi r y - 4\pi r^2\ \Delta Gv = 0 \Longrightarrow \mathbf{r'} = 2y/\Delta Gv \ldots\ldots (2)$$

Where

ΔGv: is the volume free energy,

Y: the solid/Liquid interface free energy,

r: the radius of nuclei.

2.3.1 Homogeneous nucleation

Nuclei that do not reach the critical radius and maximum energy shrink and dissolve into liquid Figure 2.9. When the temperature is low enough to allow nuclei above the critical *size,* further growth is enabled by a reduction in energy [8].

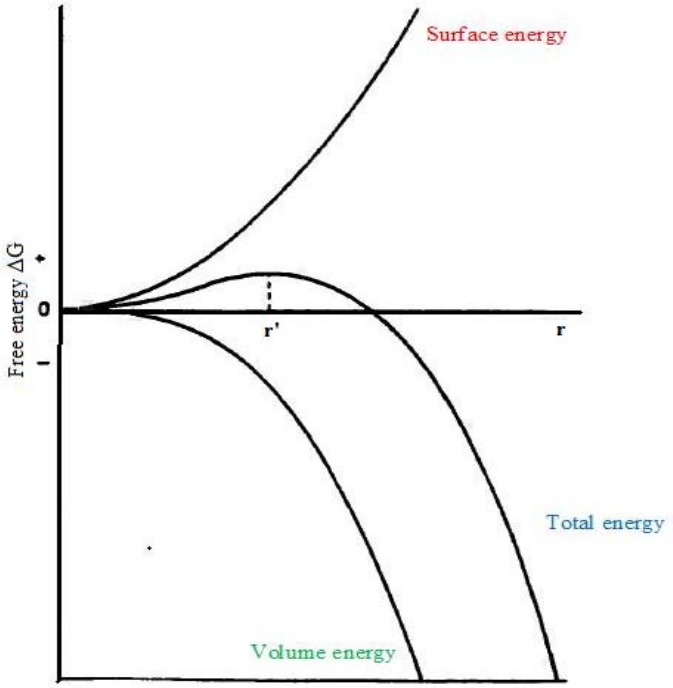

Figure 2.9: The variation of free energy with radius of nucleus is the critical radius for those nuclei which will grow

2.3.2 Heterogeneous nucleation

Heterogeneous nucleation occurs when the crystallization begins on impurities, particles, nucleation agents and mould walls. On aluminium alloy casting processes the heterogeneous nucleation communally occurs. In commercial practice, inoculating

agents are added to many molten alloys to increase nucleation sites and produce fine-grained structure. These elements are titanium and boron for aluminium alloy. While considering a solid embryo in contact with a perfectly flat mould, it can be shown that for a given volume of the solid, the total interfacial energy of the system by the following equation [8]

$$\Delta G = v\,\Delta Gv + A\gamma$$

2.4 Growth

The surface cools rapidly and heterogeneous nucleation begins on the mould wall when the liquid metal is poured into a cold mould, After nucleation, solidification process will only occur if heat is extracted through the solid, cooling the advancing front below the equilibrium freezing point. As the rate of extraction of heat increases, the temperature of the solidification front falls and the growth rate (G) increases, where *G* is defined as the velocity of the solid growing into the liquid. For pure metal as the driving force for solidification increases the planar are the series of transitions at the solidification front. With higher growth rate, cellular solidification is seen to develop. At a very high cooling rate, the cells grow rapidly and the advancing projections have cornplex tree like geometry. This type of growth is called dendritic solidification [9]

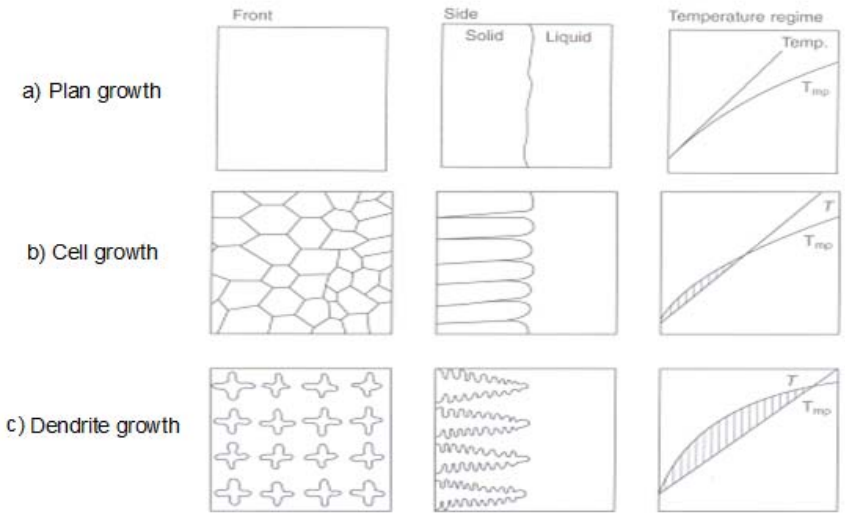

Figure 2.10: Transition of growth morphology from a) planar, b) cellular and c) dendritic, as compositionally induced undercooling increases

2.5.1 Solidification of dendrite

Because all castings must possess certain specific properties to service requirements, the relationships between the properties and structures developed during solidification are important. These sections describe the relationships in terms of dendrite morphology and the concentration of alloying elements in various regions of the casting.

The compositions of dendrites and of the liquid metal in casa the phase diagram of the particular alloy. When the alloy is cool very slowly, each dendrite develops a uniform composition. Under normal typically encountered in practice, however, cored dendrites are formed, which have surface composition that is different from that at their centers concentration gradient ,the surface has a higher concentration of alloying

elements than at the core dendrite due to solute rejection from the core toward the surface during solidification of the dendrite (known as microsegregation). The darker shading in the inerdentritic liquid near the dendrite roots shown in Figure 2.11 indicates that this region has a higher solute concentration. Consequently, microsegregation in the much more pronounced than in others.

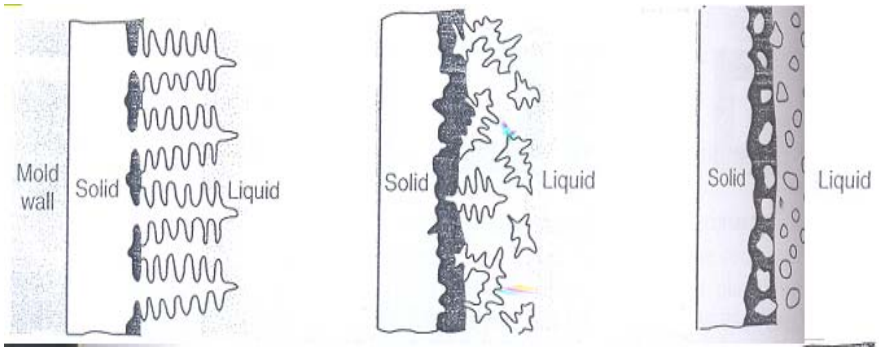

a) b) c)

Figure 2.11: Schematic illustration of three basic types of cast structures; a) columnar dendritic b) equiaxed dendritic c) equiaxed nondendritic

. The growth rate into the liquid depends on the crystal orientation, and only those that have a rapid growth direction normal to the mould wall will survive the growth process and these grains are columnar in shape. Actually, the columnar grains grow from the surface to the interior, with equiaxed grains at the centre. In this process, small pieces of the dendrite arms are separated from the dendrite and swept into the center. This happens when, the heat released at the melt/dendrite arm interface is sufficient to raise the temperature locally, thus causing the side arms to melt. These small crystals move into the center of the casting to serve as the nuclei for the formation of equiaxed grains.

During the growth, dendrite arms will knit together forming a single crystal Lattice known as a grain. The grain may include thousands of dendrites. The mechanical properties of most cast alloys are strongly dependant on secondary arm spacing. A decrease in dendrite am spacing (DAS) is accompanied by an increase in ultimate tensile strength and ductile [8]

2.5.2 Shrinkage solidification

The solidifying metal has a distinct border between the solid and liquid phases. In long freezing range alloys the contraction area are dispersed as solidification proceeds simultaneously throughout the casting. Also alloy are prone to widespread porosity such as, the solid portions are suspended within the liquid metal. The level of the liquid can fall to accommodate the volumetric contraction [10]. Generally, the grains intersect and form continues structure. Movement of liquid metal is restricted to intergranular or dendritic channels. As solidification proceeds isolated portions of liquid solidify independently and cannot be fed externally. This may result in shrinkage defects in the form of scattered porosity [9]

2.5.3 Chvorino's Rule

During the early stage of solidification a thin solidified skin begin to from at the cool mould walls, and as time passes, the skin thickens. With flat mould walls, this thickness is proportional to the square root of time. Thus, doubling the time will make the skin $\sqrt{2}$ = 1.41 times, or 41% thicker. The solidification time is a function of the volume of the casting and surface and is known as Chvorino's Rule

$$\text{Solidification time} = C\left(\frac{volume}{surface\ area}\right)^{n}$$

Where: C is constant that reflect the mold material properties including the latent heat n is typically is found to have value between 1.5 and 2 and usually taken 2 [10]

2.6 Lost Foam Casting (LFC)

.

Lost foam casting is a full mold process, which uses a polystyrene foam pattern in unbonded sand. The foam pattern is prepared by injecting expandable polystyrene beads under the combined action of steam and pressure. Then, the pattern assembly is coated with refractory slurry and dried. The coated pattern assembly is set in a steel flask, which is then filled with unbonded sand. The flask is vibrated to compact the sand. Finally, molten metal is poured directly into the mated pattern assembly. The polymer pattern undergoes thermal degradation and is replaced by the molten metal [12].

Raw polystyrene beads are expanded using heat and vacuum to a density of 1.5-1.6 lb/ft' for aluminum. The expanded bead is blown into a mould cavity and steam is passed through the mould causing the beads to expand slightly and fuse. Water is sprayed on the back side of the mould to lower the pattern temperature prior to removing it. The polystyrene patterns are coated with a refractory wash to prevent metal penetration into the surrounding unbonded sand during casting. The coatings used are silica materials in a water base. These must be dried from four to six hours at temperatures of about 65°C. Temperatures over 70°C should be avoided because the pattern may soften and become distorted. Vibration and compaction of the sand mass is usually achieved simultaneously with sand fill to prevent distortion. Figure 2.12 shows the main procedure steps in the LFC process [12].

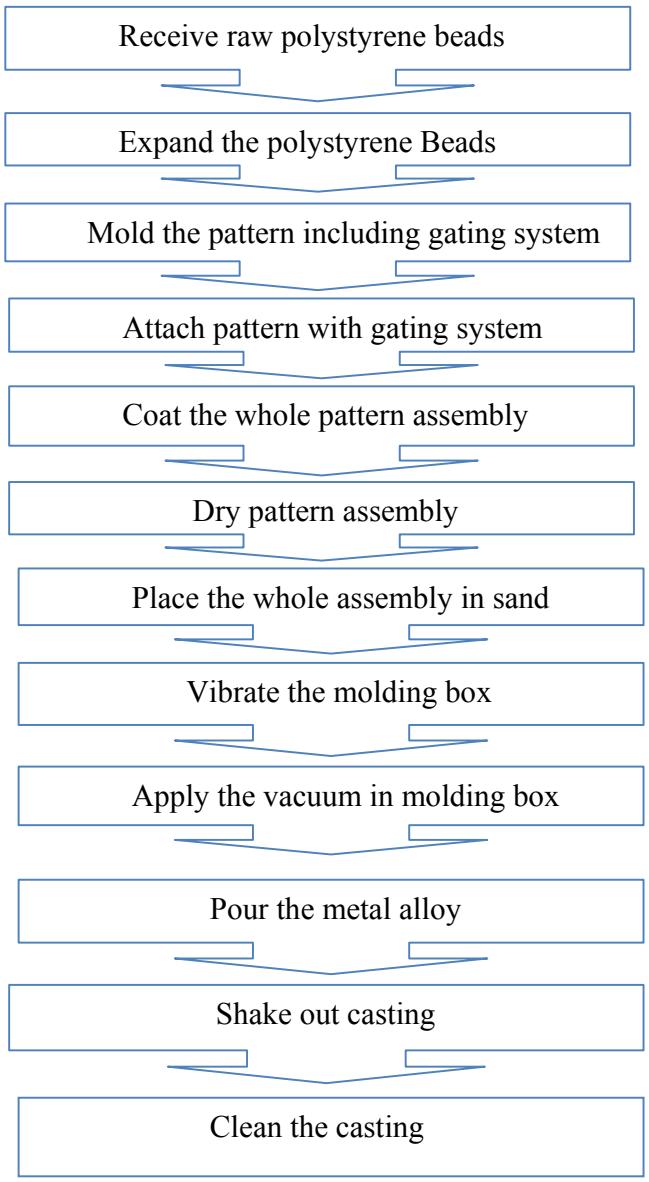

Figure 2.12: Lost foam steps

2.6.2 Preparation of bead of polystyrene

The mold of lost foam casting starts with expandable polystyrene pattern, which begins with expandable polystyrene with benzene, a derivative of crude oil and ethylene and derivative of natural gas. The ethylbenzene is converted to styrene by the chemical

removal of hydrogen. Firstly, styrene is polymerized and then expanded into beads of controlled site using pentane. Further, pre-expansion is accomplished using steam or hot air. This is carried out in an expansion machine, thus changing the density of the beads from 0.64 grlun) to 0.024-0.028 grlcm3 (for aluminium casting products), Littleton. The final product is expandable polystyrene (EPS). Other polymers such as polymethyl methacrylate (PMMA) and polyalkylene carbonate (PAC) have been used for production of ferrous castings.

2.6.3 Pattern Making

The pre-expanded beads are blown into the cavity of a split aluminium die, which is steam heated to further expand and fuse the beads. The die is cooled with water and the pattern is ejected. If complex shapes are required, different sections of the pattern may be joined with hot melt adhesive. Thus, part consolidation is a major advantage of this process. The foam pattern changes dimensions rapidly after removal from the molding machine. First, some polymer cells in the pattern undergo stress relaxation. Thereafter, equalization of gas pressure in the beads causes both pattern expansion and contraction.

2.6.4 Coating

The cluster must be coated to develop a shell between the foam and the sand. The coating material is a thixotropic liquid consisting mostly of refractories, emulsifiers and antibacterial chemicals in a water carrier. The refractories used are usually silica, alumina or zircon. Coating can be applied by dipping, spraying or pouring. Coating provides a physical boundary between the compacted sand and molten metal, prevents metal penetration and sand erosion during pouring, and allows decomposed products to

escape during degradation of foam. The refractory materials must have controlled permeable, insulating capacity, abrasion resistance, and ability to absorb the liquid pyrolysis products. The coating should have sufficient insulating properties to prevent freezing in thin-walled casting before the pattern can be displaced. The permeability of the coating is the key to control the rate of removal of the products of pyrolysis from the mold.

2.6.5 Sand filling and vibration , compaction

During the sand filling, the flask is vibrated periodically to compact the sand and to ensure that the sand is wrapped tightly around the cluster and fills al1 internal cavities of the pattern. Compacting is achieved by using a vibrating table that has motors with off centre counter rotating weights. The sand must allow the products of pyrolysis to escape provide mechanical support to the pattern during pouring and prevent metal penetration. The sand often used in LFC is silica (SiO2) with grain fineness number (gfn) of 25-45. An alternative mold material recently used in the LFC industry is synthetic mullite (3Al2O3, 2Si02). This material has low thermal expansion and thermal conductivity compared to silica, thus enhancing dimensional stability and fallibility of the liquid metal in complex parts,

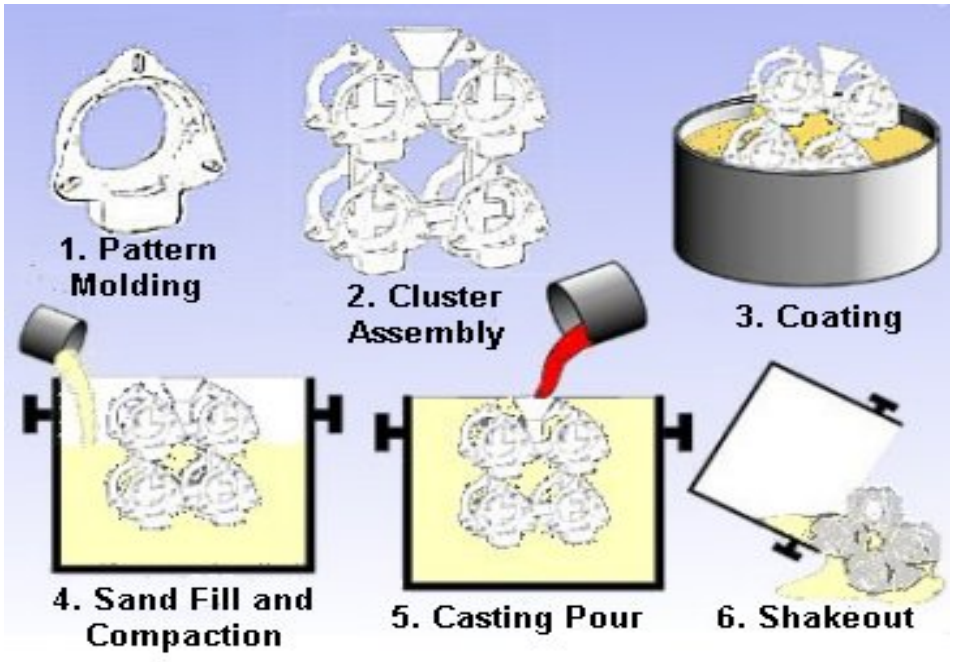

Figure 2.13: Lost foam process

2.6.6 Lost Foam Filling Mechanism

In the lost foam casting the pattern degrades in the liquid and the gas products escape into the loose sand after the molten metal is introduced and the metal then fills the foam pattern to achieve the target casting. During the pyrolysis process gas layer exists between the metal and the polymer front [13]. This gas layer predominantly consists of primary thermal degradation product of styrene. The advancing metal front first melts and partially vaporizes the polystyrene. As explained, the small gap between the molten metal front and EPS is filled with a mixture of gases (mostly styrene monomer), and liquid styrene. The gases quickly escape through the permeable coating and the liquid may be absorbed into the coating or may form a thin liquid residue between the casting and the coating. This liquid residue causes the coating to blacken and often leaves a layer of carbon between the casting and the coating. The amount of liquid and gases produced by ablation of EPS depends on the molten metal filling temperature and the foam density [16]. Figure 2.14 schematically shows the molten metal front in LFC.

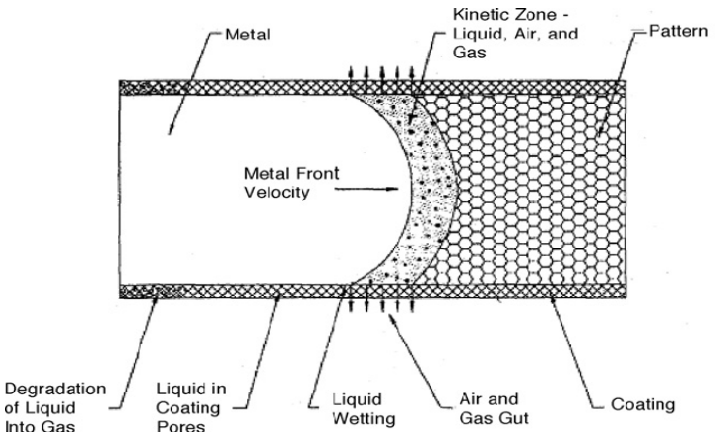

Figure 2.14: Schematic of molten metal front in LFC .

2.7 Parameters affecting LFC

There were many studies which focused on the process parameters affecting the quality of casting structure and mechanical properties. The following are some of these factors:

2.7.1 Degree of vacuum

The expandable polystyrene (EPS) pattern is a key feature of EPC process which is buried in unbonded sand and replaced by molten metal. Sudhir Kumar *et al.* in 2006 used the effect of process parameters like degree of vacuum, pouring temperature, sand grain finesse number, amplitude of vibration and time of vibration on the surface roughness of Al–7% Si alloy castings in EPC process. They wanted to evaluate the effect of selected process parameters, and used the response surface methodology (RSM) to formulate a mathematical model which correlates the independent process parameters with the desired surface roughness. The central composite rotatable design has been used to conduct the experiments. They found that the surface roughness

increases with increase in degree of vacuum, pouring temperature. Whereas, it has an inverse relationship with sand grain finesse number, amplitude of vibration and time of vibration [17].

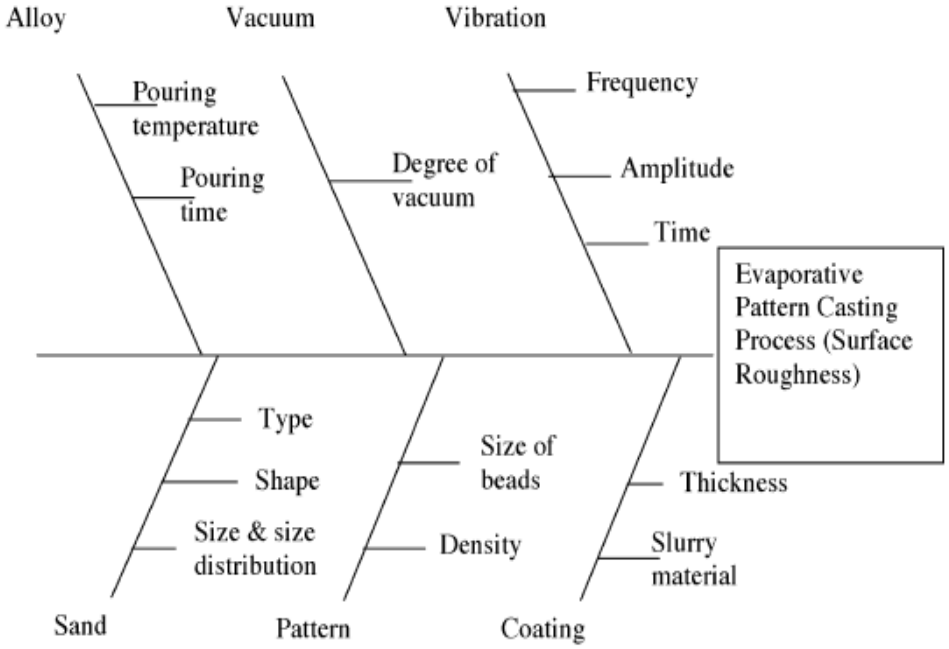

Figure 2.15: Ishikawa cause effect diagram of LFC process

2.7.2 Permeability pattern coatings

Firstly, the coating allows the retention of the shape of the mould cavity in the gap between the receding degradation front of the pattern and the advancing liquid metal filling the mould. Secondly, because it is permeable, the degradation products of the pattern can pass through it. W. D. Griffiths P. J. Davies in 2007 studied the permeability of lost foam pattern coatings for Al alloy castings. They found the permeability of typical pattern coatings for the lost foam casting of Al to vary from about 0.1 Darcy, (10-13 m^2), for a low permeability coating, to about 1 Darcy (10-12 m^2), for a high permeability coating. Permeability reduced by increasing coating thickness [19].

2.7.3 Pressure

Porosity is thought to be severe in aluminium alloy castings produced by lost foam process due to the pyrolysis of the polystyrene foam pattern during pouring, which affect the mechanical properties. Bokhyun *et al* reported that to eliminate porosity is to apply high pressure to the molten metal like an isostatic forging during solidification. Fundamental experiments were carried out to evaluate the effect of the external pressure on the porosity and mechanical properties of A356.2 alloy bar in the lost foam casting. They found that the solidification time and porosity decreased with increasing the applied pressure during solidification. Applying external pressure was effective in decreasing the porosity and increasing the elongation of the lost foam casting [20].

2.8.4 Pouring temperature

In studying the effect of pouring temperature on the morphology of primary Al particles and the rheological behaviour of microstructures for semi-solid Al–Si 356 alloy, Omid Lashkari *et al* (2006) reported stated that dendrite primary Al structures formed at the highest pouring temperatures of 675–695 ◦C have the greatest viscosity numbers. They are almost two orders of magnitude greater than those for rosette structure formed at moderate pouring temperatures of 630–645 ◦C. The viscosity of the dendrite primary Al structures is three orders of magnitude greater than those for globular morphology formed at the lowest pouring temperature of 615 ◦C [21].

CHAPTER 3

RESEARCH METHODOLOGY

3.1 Introduction

Proper experimental plan is necessary to achieve good results in conducting research. This chapter describes the experimental setup, measurement techniques and measurement equipment used in this study. Figure 3.1 shows the steps of experimental work.

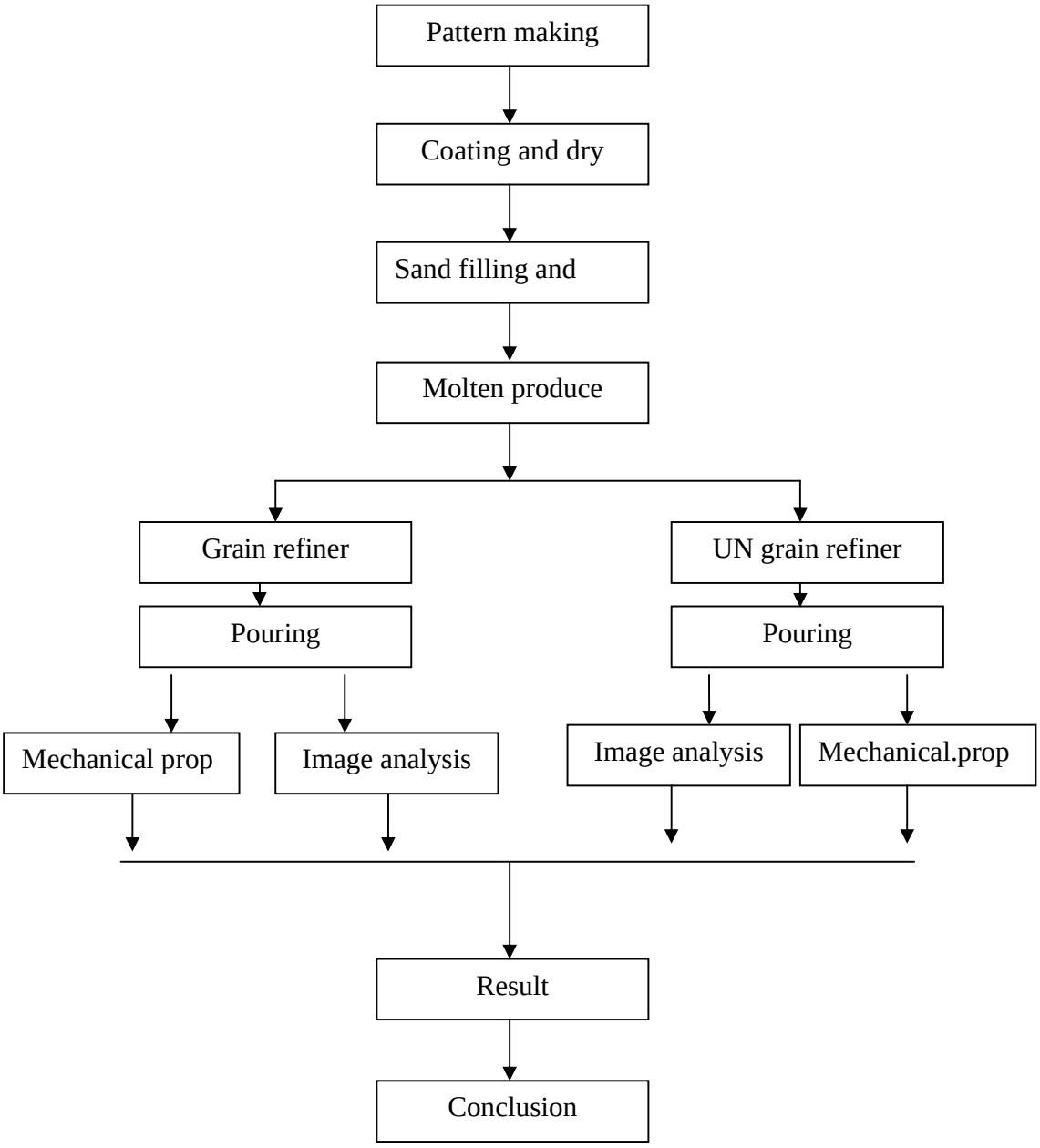

Figure:3.1 experimental steps

3.1.1 Pattern making

The pattern design is a step-like shape 150x250 with 3, 6, 12, 18, 24 mm thickness (Figure 3.2 and 3.3). The riser was made with dimensions: 24x38x36 mm with a extra added foam on top. The molds were cut using hot wire with accuracy of 0.5 mm. The foam density used was 16, 20, and 32. Two categories of castings were produced: 5 castinsg in unmodified condition but poured at five different temperatures: 700, 720, 740, 760 and 780 ^{o}C. The other five castings were made at the same pouring temperatures but the melt was grain refine by the addition of AlTiB grain refiner. The riser was assembled by polystyrene glue.

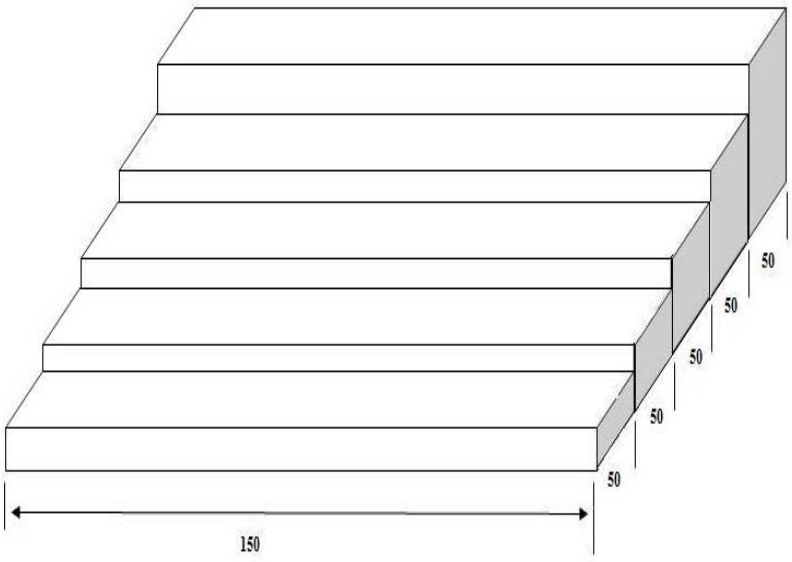

Figure 3.2: Pattern dimensions

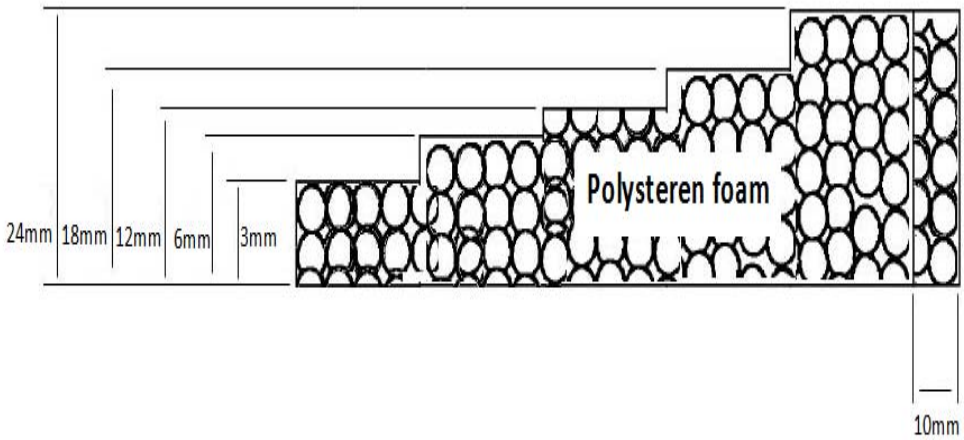

Figure 3.3: Sections of the pattern

3.1.2 Pattern coating and drying

The refractory coating used is Zircon coating ZR-A. It was mixed with colloidal silicate (Figure 3.4). The viscosity of the coating was 27 measured by flow cup in order to get the desired coating thickness of 0.3-0.5 mm. The foam was dipped in the refractory slurry and shaken to drip dry. The ratio for the colloidal silicate to the zircon flour is 1:4. 100g of colloidal silicate added with 400g of zircon flour. Using flow cup (Figure 3.5) . The time for the slurry to flow-out from it is set to be 27 seconds. The insulating characteristic of the coating reduces heat transfer from the liquid metal to the sand mold, thereby increasing the flow length of the liquid aluminium alloy and improving castability. The refractory slurry should have the appropriate viscosity to cover the surface of the foam cluster. The coated patterns are then placed for 6 hours in a dry place at a temperature of 60ºC (± 1ºC) (Figure 3.6).

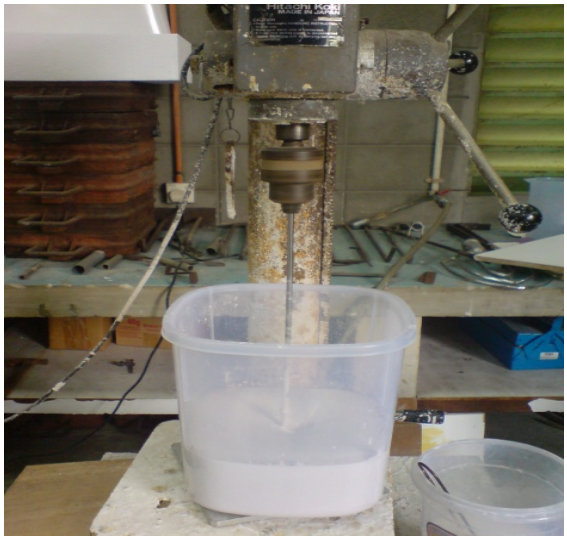

Figure:3.4:coating mixer

Figure3.5: flow cup

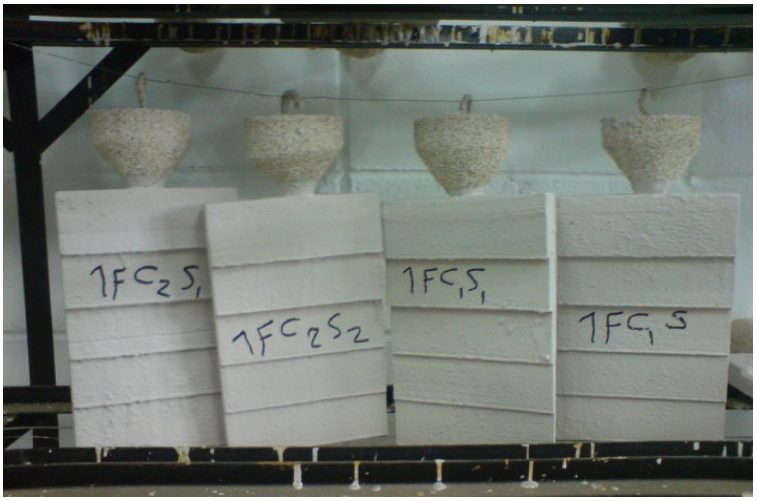

Figure3.6: patterns after coating

3.1.3 Sand filling and vibration

The sand material used is of standard AFS grain fineness number is silica sand (SiO_2) of 35 (gfn). Sand is slowly introduced into the flask by hand and the filling is accomplished by gravity. Uniform vibration of the flask is facilitated by a 4- point clamping of the flask to the vibration table. Actual vibration was carried out by two off-center motors with counter weights (Figure 3.7). The flask was thus subjected to a horizontal vibration for 3 minutes during the sand filling process.

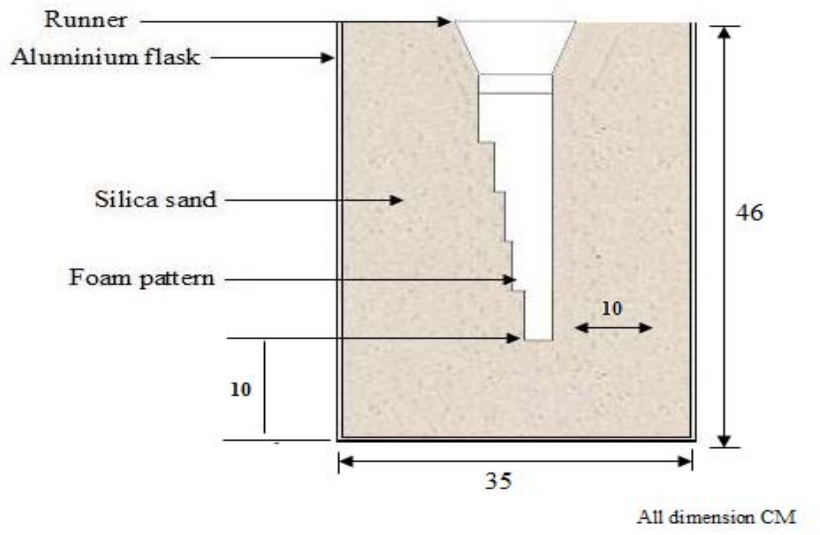

Figure 3.8:. Flask position

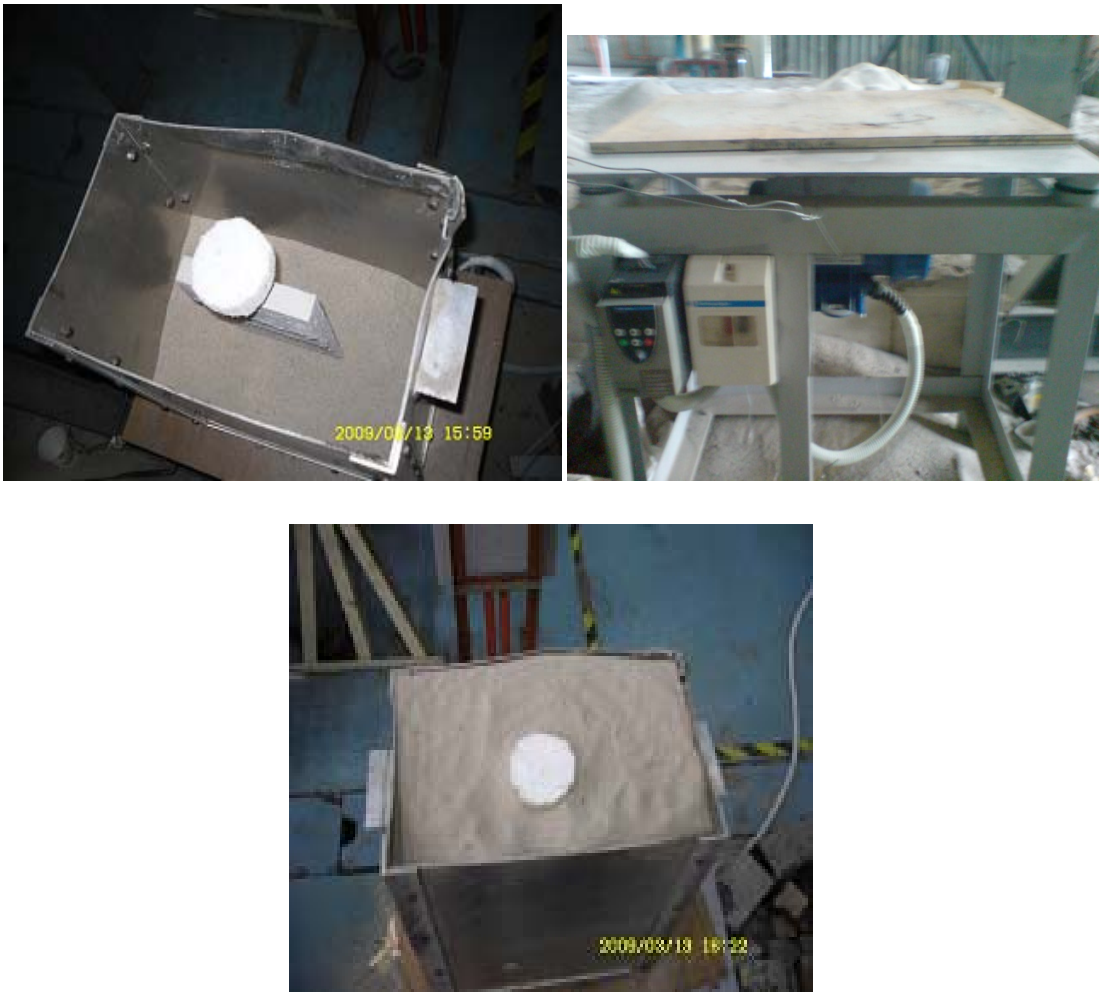

Figure 3.7: sand filling and vibration

3.1.3 Temperature measurement

Individual thermocouple wires (type k, 26 gauges) were inserted into the ceramic Insulator tube. The positive and negative ends of two such wires were welded to form the couple and the thermocouple tip was inspected for proper weld. They were tested at 100 ^{o}C in boiling water to determine their temperature measurement accuracy. Then the thermocouple was dipped inside the molten metal to measure the temperature.

3.1.4 Melting procedure and casting

The metal was LM6 alloy with the chemical composition as in Table 3.1

Element	Si	Fe	Mg	Mn	Cu	Ti	Zn	Other
Wight%	10-13	0.06	0.1	0.5	0.1	0.2	0.1	Max 0.15

Table 3.1: Chemical composition of LM6 Alloy

Melting of the LM6 alloy was made in an induction furnace (Figure 3.9) and pouring made at the following temperatures: 780,760,740,720,700 (±5). The grain refiner titanium-boride (TiB) was introduced into the melt as AlTiB master alloy. Once the LM6 is melted the refiner (0.2% AlTiB) was wrapped in an aluminium foil and then inserted deep in the bottom of the melt using a shaft. TiB is practically used to improve many metallurgical properties such as resistance to cracking, ductility and surface finishing characteristics in addition to refining the grain size.

Figure 3.8: Shaft used to mixed the TiB

Figure 3.9: induction furnace

Figure 3.10: Pouring of castings

3.2 Analysis

3.2.1 Casting analysis

3.2 After solidification, the castings were removed and analysed in terms of

- Surface condition
- Casting filling and/ or misrun
- Coating penetration
- Porosity

Prior to casting the samples, preliminary work was carried out using three different foam densities of 16, 20, and 32. The purpose from these preliminary trials was to identify which foam density is suitable for lost foam casting of LM6.

3.2.2 Microstructure Analysis

3.2.2.1 Sample preparation

For microstructure analysis the samples were cut from both ends of the castings as shown in Figure 3.11. Then all samples were mounted, grinded, polished and finally etched for analysis according to standard metallographic procedures.

A total of 50 samples were collected from different sections at different temperatures. Etching of the samples was mad using Keller's reagent (HF, HCL, HN03 and Hz0 in equal parts) for 15 seconds.

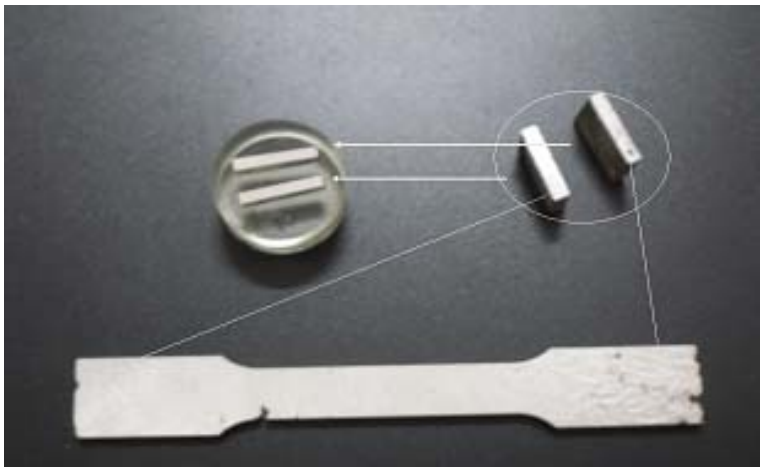

Figure 3.11:Sample preparation for microstructure analysis

3.2.2.2 Image Analysis (Eutectic Spacing Measurements)

Eutectic spacing measurements were made on the same samples used for microstructure analysis. The linear measurement technique was used on micrographs at a magnification of 100X as shown in Figure 3.12. The final results of the spacing are the average of at least 10 measurements.

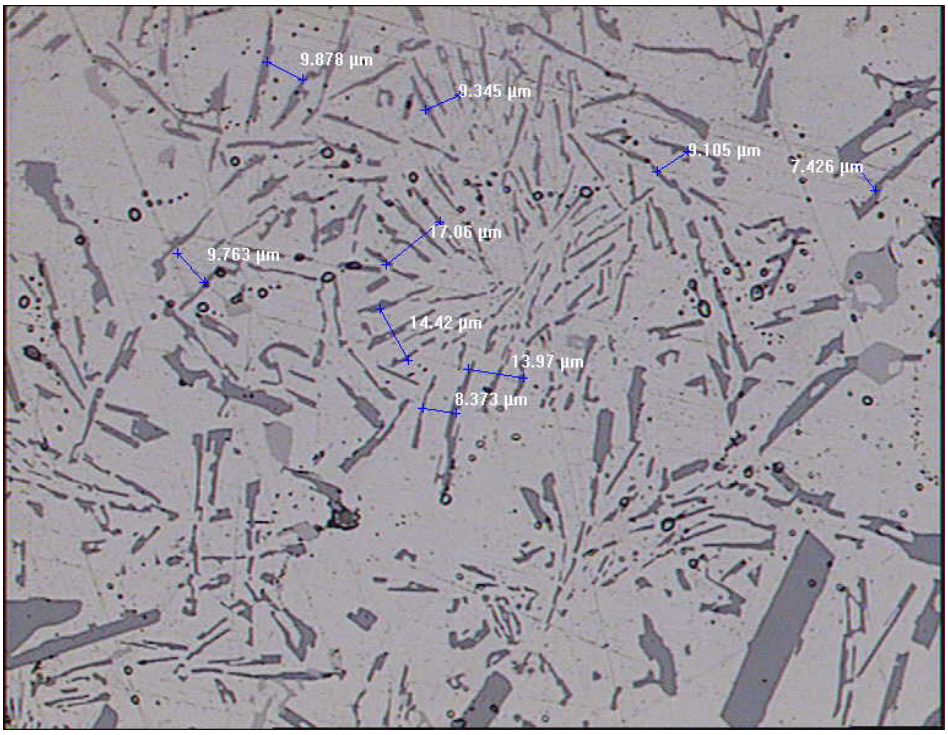

Figure 3.12:Method showing the measurement of eutectic spacing

3.2.3 Mechanical properties

3.2.3.1 Tensile test

Tensile testing was conducted on specimens machined according to A376 ASTM standards (Figure 3.13). The main properties measured included ultimate tensile strength, yield strength and percent elongation. Tensile testing was conducted on selected castings with different thickness sections and cast at different pouring temperatures.

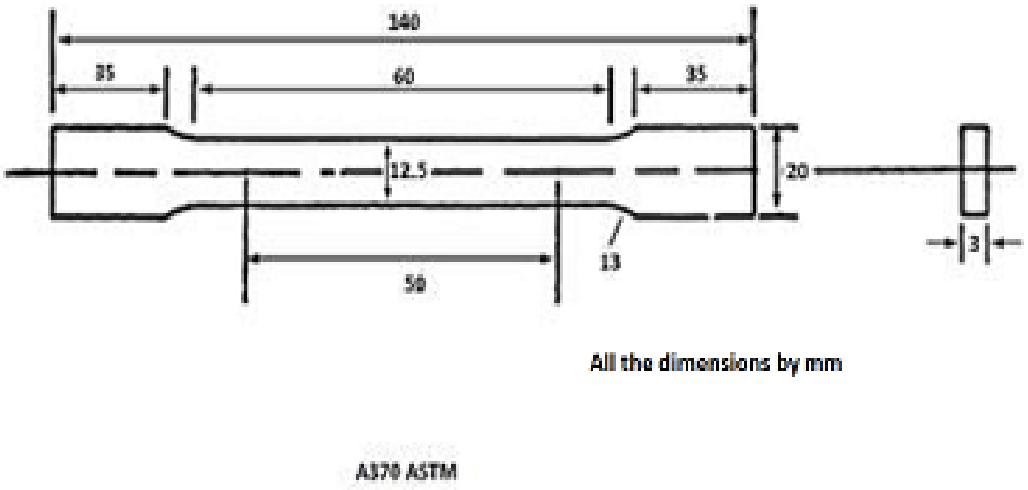

Figure 3.13: Tensile specimens test dimensions

TENSILE STRENGTH versus BRINELL HARDNESS

Aluminum alloys, 5xxx series (major alloying element-magnesium)
Temper: H (strain-hardened). Hardness range (36-105) HB measured at 500-kgf load

$\sigma = 604 \times HB - 2580$

Brinell hardness *HB, X*	Tensile strength, psi σ, *Y*	*XY*	X^2	Y^2	Parameters of the regression line *slope*	*intercept*	Correlation coefficient
36	20000	720000	1296	400000000	604	-2580	0.991
40	23000	920000	1600	529000000			
41	23000	943000	1681	529000000			
46	25000	1150000	2116	625000000			
46	26000	1196000	2116	676000000			
48	26000	1248000	2304	676000000			
50	28000	1400000	2500	784000000			
51	29000	1479000	2601	841000000			
55	30000	1650000	3025	900000000			
60	33000	1980000	3600	1.089E+09			
60	33000	1980000	3600	1.089E+09			
62	36000	2232000	3844	1.296E+09			
63	35000	2205000	3969	1.225E+09			
63	35000	2205000	3969	1.225E+09			
67	39000	2613000	4489	1.521E+09			
67	39000	2613000	4489	1.521E+09			
68	38000	2584000	4624	1.444E+09			
68	38000	2584000	4624	1.444E+09			
70	38000	2660000	4900	1.444E+09			
73	40000	2920000	5329	1.6E+09			
73	40000	2920000	5329	1.6E+09			
73	40000	2920000	5329	1.6E+09			
73	40000	2920000	5329	1.6E+09			
73	42000	3066000	5329	1.764E+09			
73	42000	3066000	5329	1.764E+09			
75	41000	3075000	5625	1.681E+09			
77	42000	3234000	5929	1.764E+09			
77	42000	3234000	5929	1.764E+09			
78	45000	3510000	6084	2.025E+09			
78	45000	3510000	6084	2.025E+09			
80	48000	3840000	6400	2.304E+09			
80	48000	3840000	6400	2.304E+09			
81	44000	3564000	6561	1.936E+09			
90	51000	4590000	8100	2.601E+09			
100	60000	6000000	10000	3.6E+09			
105	63000	6615000	11025	3.969E+09			
2347	1327000	94266000	166129	5.356E+10			

Table 3.2 TENSILE STRENGTH & HARDNESS

3.2.3.2 Vickers Hardness

Hardness testing was performed on the same samples used for microstructure analysis using Vickers hardness testing machine. The hardness values are the average of 5 readings.

CHAPTER 4

RESULTS AND DISCUSSION

4.1 Introduction

This chapter describes all the findings from this research. Microstructure analysis, the results of the eutectic spacing, hardness, and tensile test result for different sections cast at different pouring temperatures. The different section thickness and pouring temperatures allow the production of different cooling rates.

4.2 Casting analysis

After solidification, the castings were removed and analysed in terms of

- Surface condition

- Casting filling and/ or misrun
- Coating penetration
- Porosity

The results of the preliminary castings using the three different foam densities of 16, 20 and 32 kg/m^3 are presented first. As shown in Figure 4.1a and Figure 4.1b, castings produced the foam densities of 16 and 32 are have very poor appearance and two sections (3 and 6 mm) not filled. At the castings conditions used it was very difficult to obtain complete castings using these two densities.

When a foam density of 20 was used, there were many improvements as shown in Figure 4.1c. From these preliminary castings it was decided that a foam density of 20 will be used for all castings to investigate the effects of pouring temperature and melt treatment.

Figure 4.1: Castings using 16, 20 and 32 foam density

4.3 Microstructure Analysis

Figure 4.2 and Figure 4.3 show the microstructures of the untreated, TiB-treated LM6 alloy castings for 3, 12 and 24 mm sections and poured at two different temperatures of 700 and 780^{o}C respectively. As expected, it can be observed that for a given section the microstructure becomes finer with the addition of the TiB grain refiner. This observation will be confirmed when the results of the eutectic silicon spacing are presented in the next section. The effect of pouring temperature is also evident as castings produced from higher pouring temperature of 780^{o}C were coarser compared with those cast at 700^{o}C. This is also obvious as casting at lower pouring temperature results in faster cooling rates and hence finer microstructure.

The effect of adding the grain refiner is also illustrated in Figure 4.4 which shows the microstructures of castings poured at a constant temperature of 780^{o}C for the 3, 12, and 24 mm sections with and without the addition of TiB grain refiner. It is again clear that for the same conditions the castings with TiB refiner showed finer structure compared to those untreated and that with increasing the section thickness from 3 to 24 mm also results in coarsening of the structure as thicker sections solidify at a slower rates compared to thinner sections.

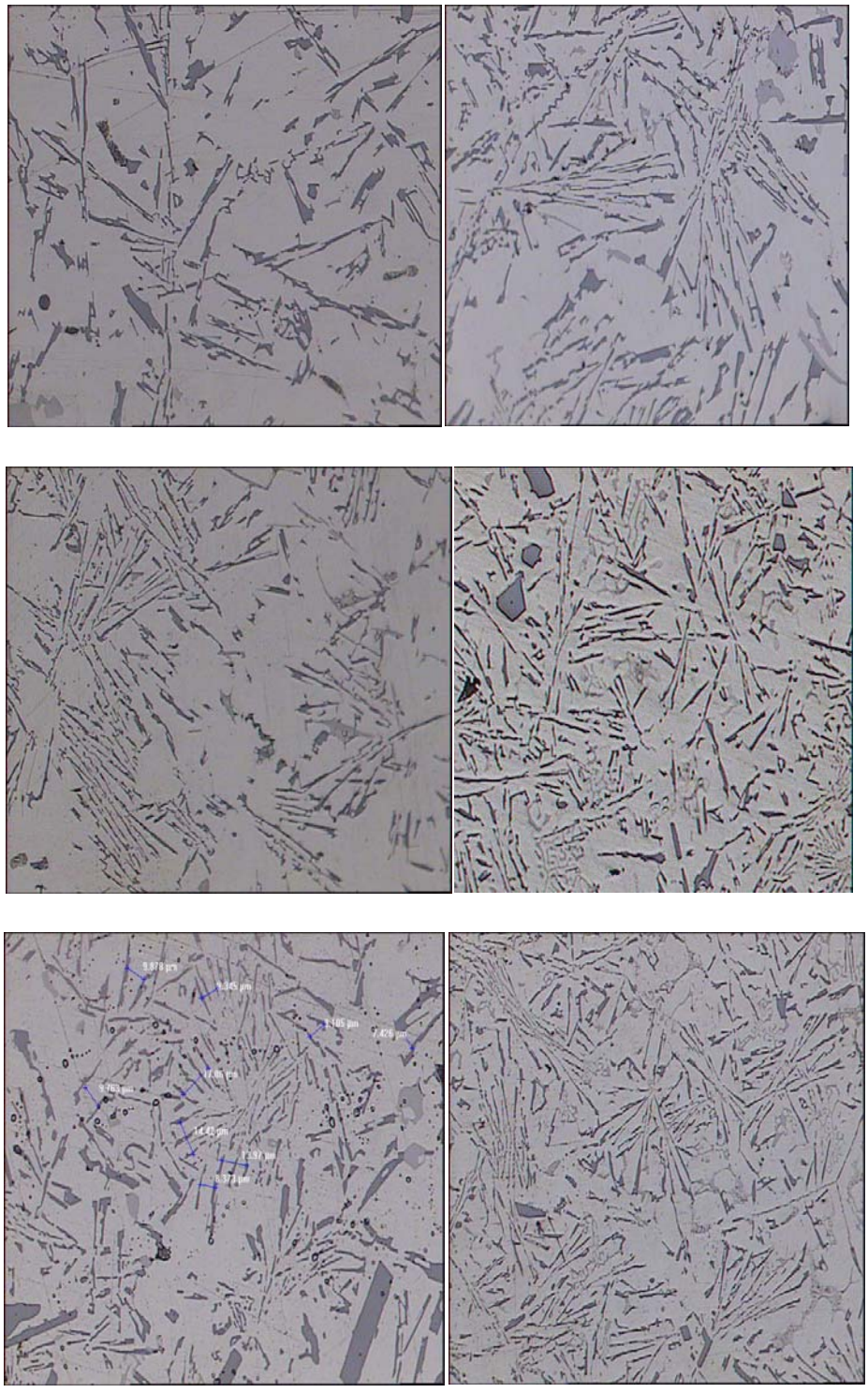

Figure 4.2: Effect of pouring temperature on microstructure on untreated LM6

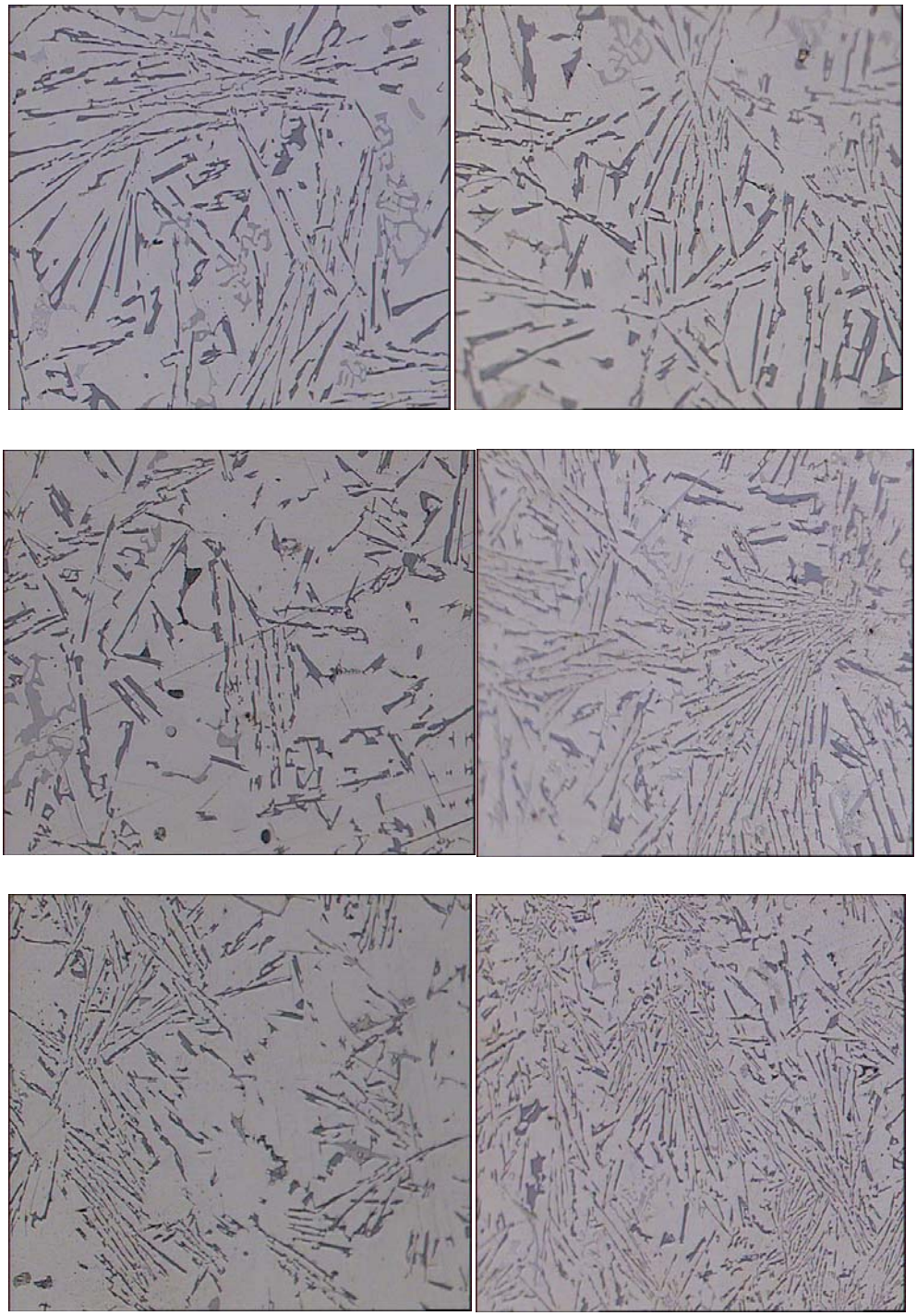

Figure 4.3: Effect of pouring temperature on microstructure on TiB-treated LM6 alloy

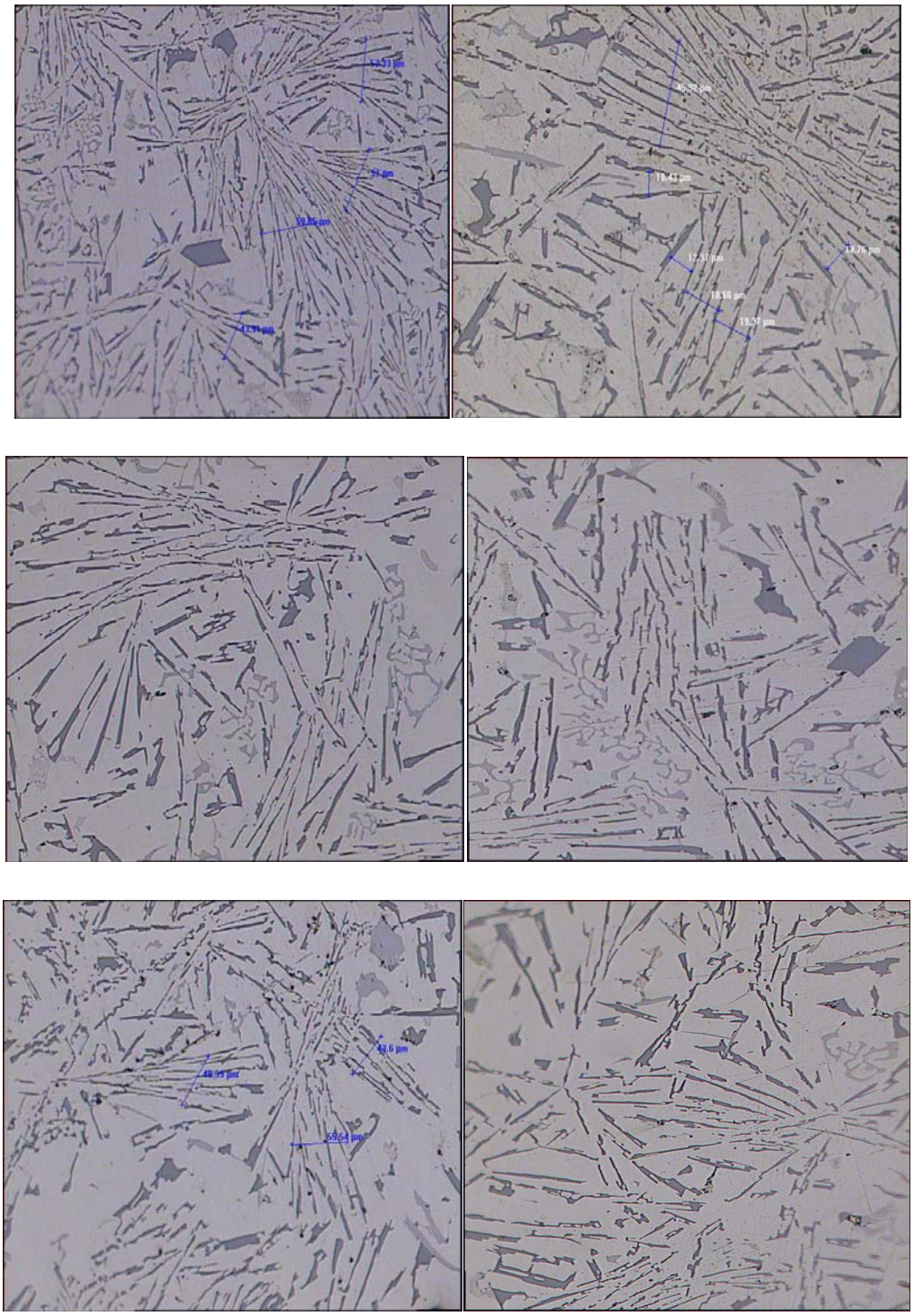

Figure 4.4: Effect of pouring temperature on microstructure on untreated and TiB-treated LM6 alloy cast at 740C° for 3, 12 and 24 mm sections.

4.4. Eutectic Silicon Spacing

The results of the measured eutectic silicon spacing are illustrated in Figure 4.5 through to Figure 4.10 for 3, 12, and 24 mm sections for unmodified and grain refined castings as function of pouring temperature. It can be clearly seen from these figures that the eutectic spacing increases with increase in the temperature due a decrease in the cooling rate and hence coarser structures are obtained at higher pouring temperatures.

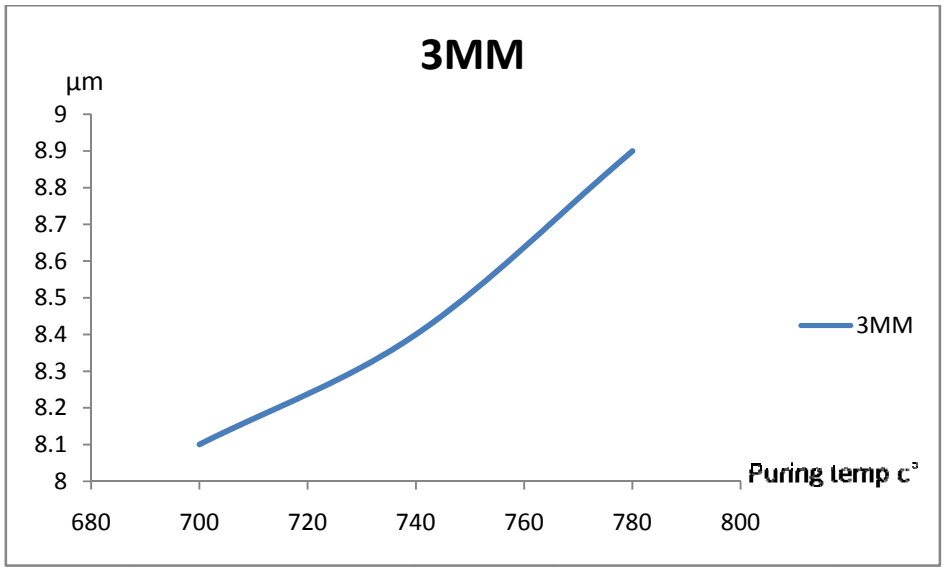

Figure 4.5: Effect of pouring temperature on eutectic spacing in 3mm thickness (fast cooling rate) for unmodified casting

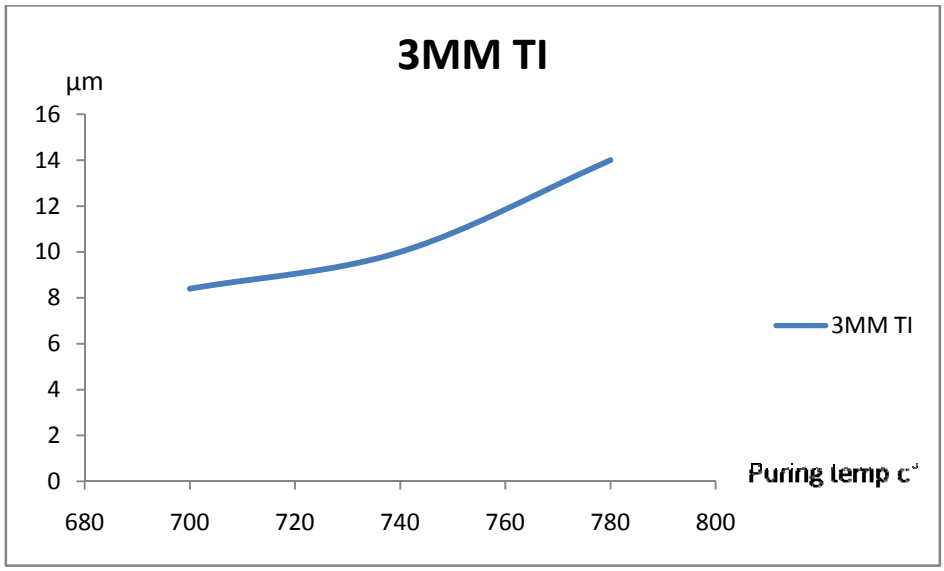

Figure 4.6: Effect of pouring temperature on eutectic spacing in 3mm thickness (fast cooling rate) for grain refined casting

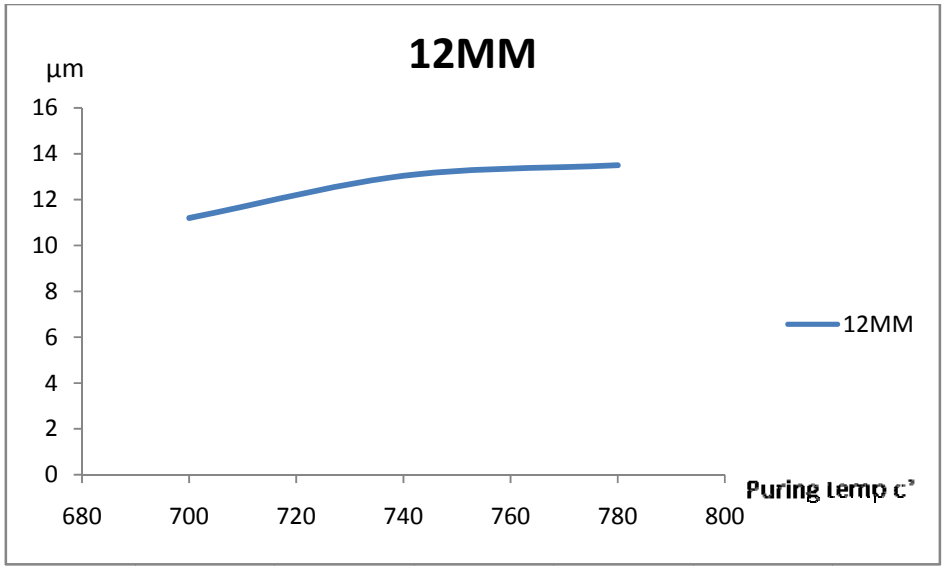

Figure 4.7: Effect of pouring temperature on eutectic spacing in 12mm thickness for unmodified casting

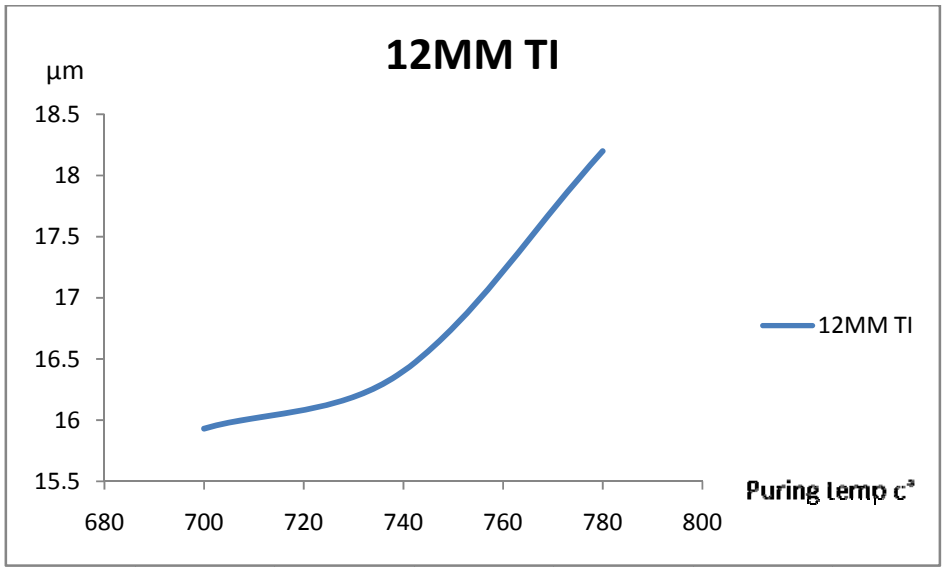

Figure 4.8: Effect of pouring temperature on eutectic spacing in 12mm thickness for grain refined casting

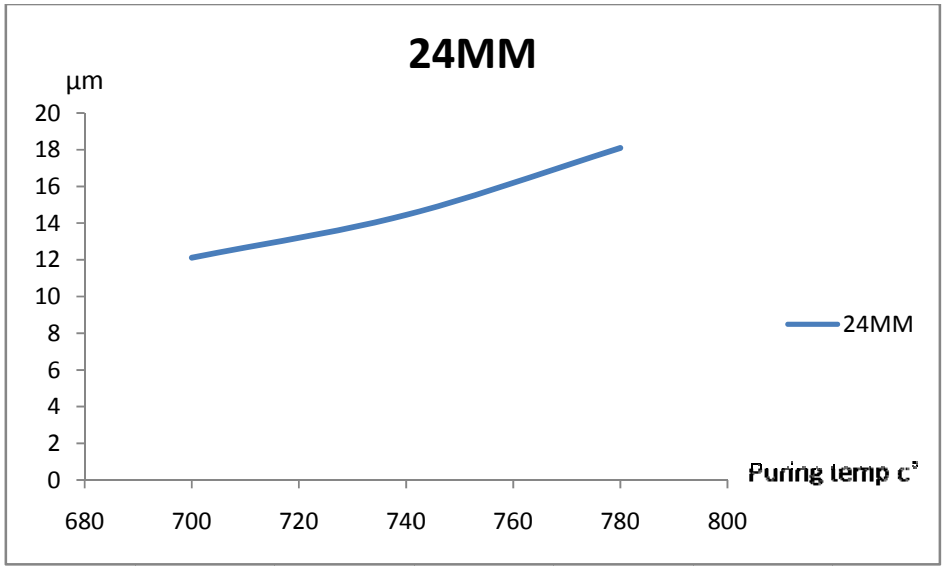

Figure 4.9: Effect of pouring temperature on eutectic spacing in 24mm thickness (lower cooling rate) for unmodified casting

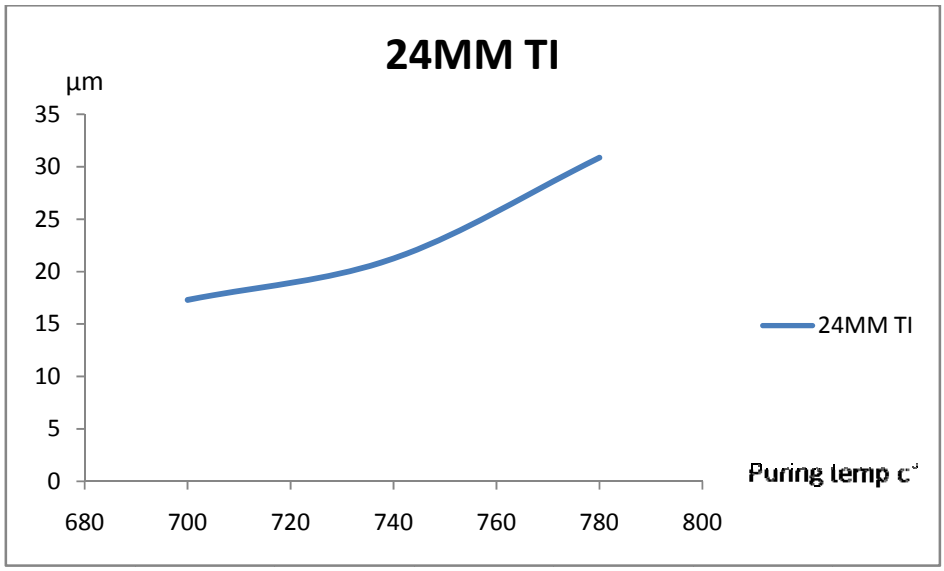

Figure 4.10: Effect of pouring temperature on eutectic spacing in 24mm thickness (lower cooling rate) for grain refined casting

To account for the effect of section thickness and grain refiner on the eutectic spacing the above figures are plotted altogether in Figure 4.11. With decreasing section thickness the eutectic spacing decreases as shown by the results of 3 mm and 24 mm for example. This is due to the fact that thinner sections will solidify faster and produce finer structures whereas thicker sections solidify at slower rates and produced coarser structures.

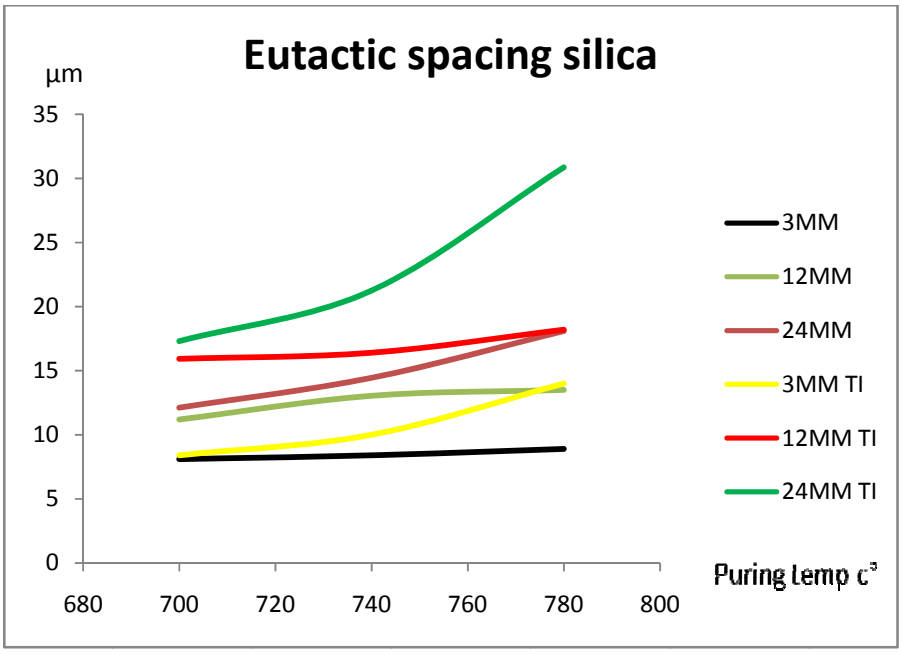

Figure 4.11: Effect of pouring temperature, section thickness and grain refiner on eutectic spacing

4.3 Mechanical properties

4.3.1 Hardness test

As shown in the Figure 4.12 the maximum hardness was obtained in the thinner sections (3 mm) for both unmodified and grain refined castings. The effect of pouring temperature on hardness values is also shown in Figure 4.12 and it is also evident as the temperature increases the hardness decreases and the microstructure becomes coarser (eutectic spacing increases as shown in Figure 4.11)

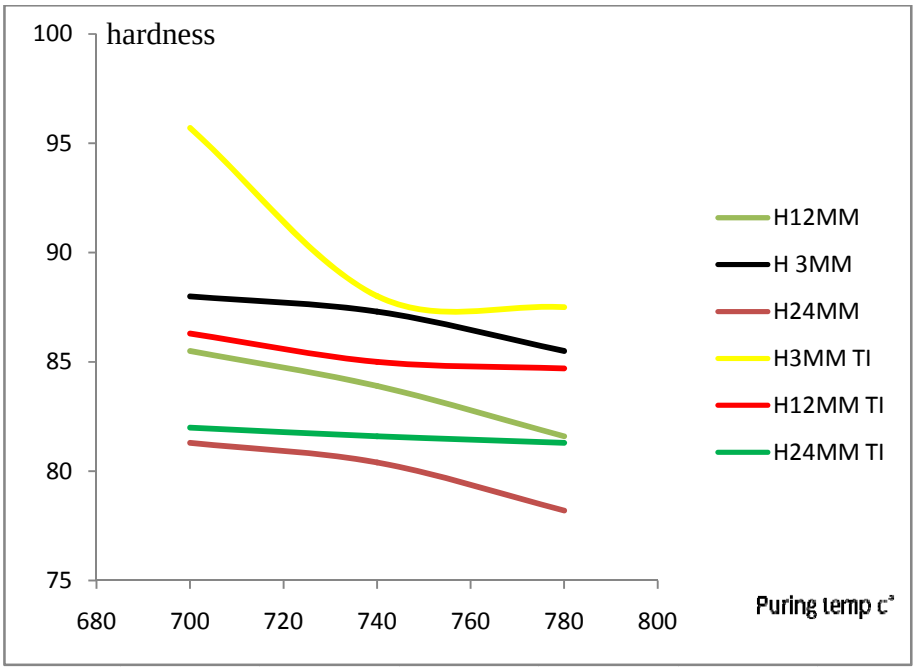

Figure 4.12: Effect of pouring temperature on hardness

4.3.2. Tensile test

As shown from the experiments the results of tensile strength are lower than expected (Figure 4.14). That is attributed to the presence of defects inside the casting along the length of the tensile test specimens. Some of these defects which include porosity are shown in Figure 4.13.

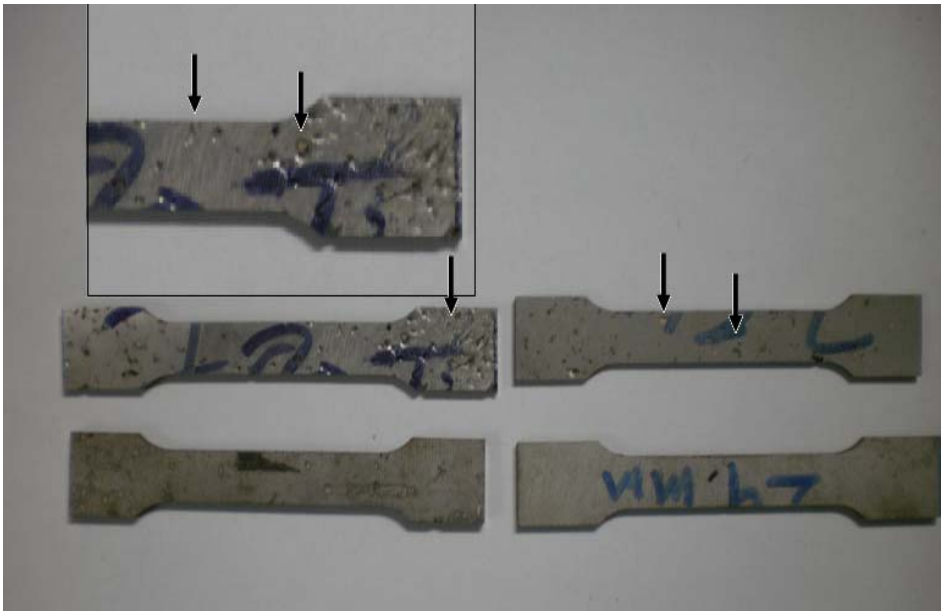

Figure 4.13: Some of the defects observed in the castings (gas porosity, penetrate of coating into the metal and shrinkage)

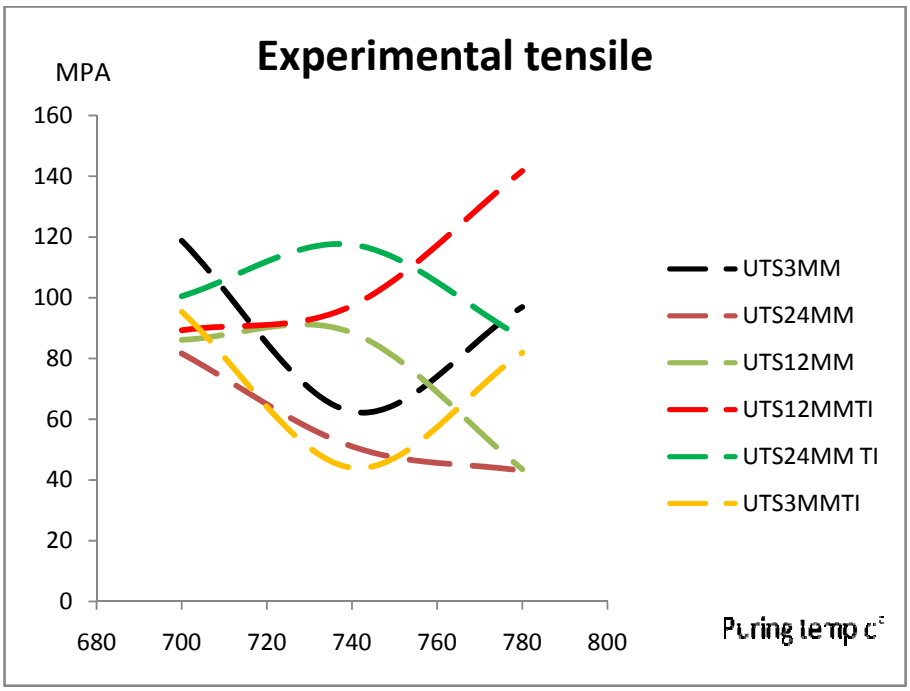

Figure 4.14: Effect of pouring temperature on experimental tensile strength

Because of the presence of these defects an attempt was made to compare the different pouring temperature on tensile properties using the theoretical tensile strength obtained by converting the hardness values using the table shown in Figure 3.2 in chapter 3. As shown in Figure 4.15 the theoretical tensile strength values are higher than those obtained from the experimental testing due as mentioned above to the presence of defects. Also the results showed the same trend as with the hardness values, that with increasing pouring temperature and decreasing section thickness the tensile strength (theoretical) increases (Figure 4.16). Similar to the experimental results the tensile strength also increases with the addition of grain refiner.

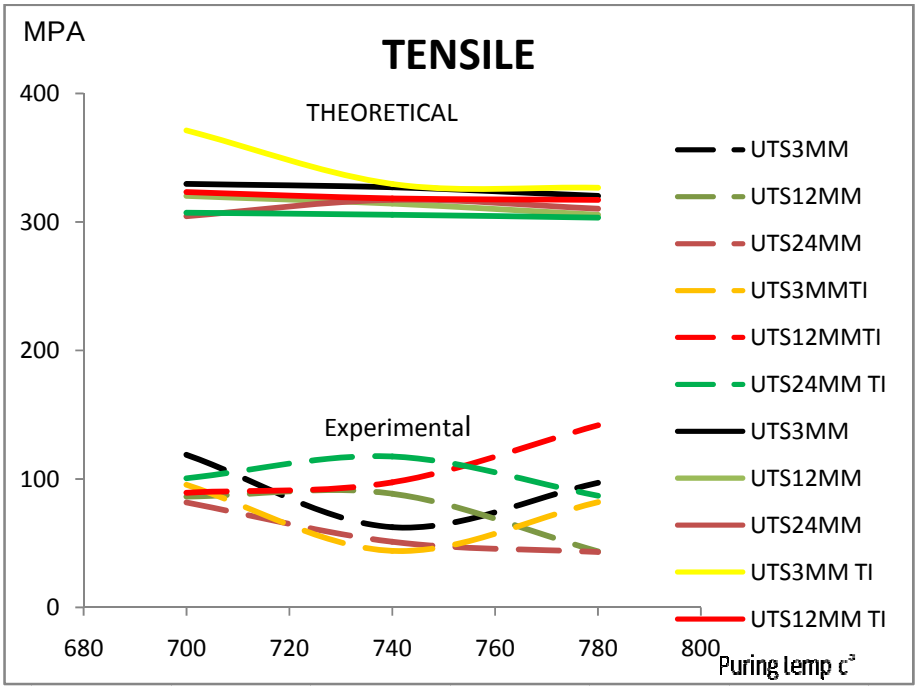

Figure 4.15: Comparison of experimental and theoretical tensile strength as function of pouring temperature

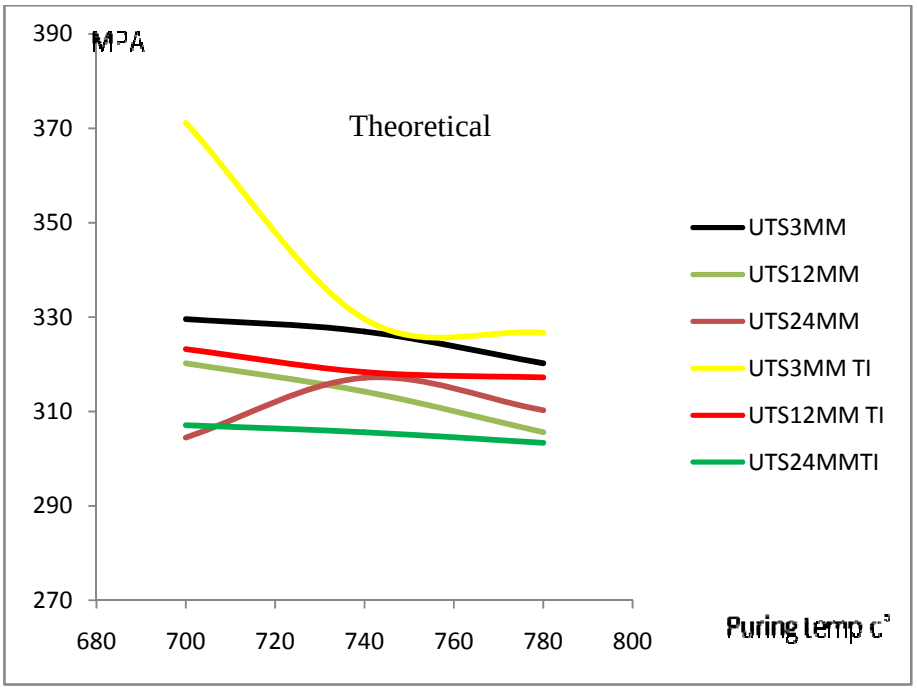

Figure 4.16: Effect of pouring temperature on theoretical tensile strength

CHAPTER 5

CONCLUSIONS AND FUTURE WORK

5.1 Conclusions

The objective of this research was evaluating the effect of pouring temperature of grain and un grain refiner Al-Si LM6 lost foam casting. Microstructure (eutectic spacing silicon), mechanical properties (tensile, hardness) are used as the performance measures. Based on this research, the following conclusions were down:

1- Successful LFC of LM6 Al-Si alloy can be achieved if the process parameters are closely controlled

2- In the present work, it was shown that foam density, pouring temperature and melt materials are controlling factors in LFC process of LM6 alloy

3- Presence of defects such as porosity, coating penetration resulted in lower tensile strengths.

4- Addition of TiB as grain refiner did not affect the castings produced significantly.

5- By increase the pouring temperature the eutectic spacing silicon increasing. The increasing of eutectic silicon spacing concurrent with increase of cooling rate (thickness).

6- The hardness decreasing with increase of pouring temperature. Also increase with fast cooling rate.

7- By lower pouring temperature and fast cooling rate we can get good casting if there are not any defects found.

5.2 Recommendations for future work.

- The effects of different sand grain size and coating thicknesses on the fluidity of liquid metal can be investigated.
- Control of penetration of coating into metal can be investigated.
- Investigate applied pressure on quality of LFC casting.
- The effect of sand vibration on permeability of gassing.

REFERENCES

1- Manufacturing processes for engineering materials (serope kalpakjian, stev R.schmid) fifith edition.

2- Aluminum Cylinder Block for General Motors Truck/SUV Engines(AFC 2007)

3- Kiyoung KIM)yand Kyongwhoan LEE. Effect of Process Parameters on Porosity in Aluminum Lost Foam Process(No.5, 2005)

4- Jun Wanga,b, Shuxian Heb, Baode Sunb, Qixin Guoa, Mitsuhiro Nishioa((2003) 29–34)

5- S Thompson; S L Cockcroft; M A Wells .Advance light metals casting development: soldification of aluminium alloy A356(pg. 194. 2004)

6- Francisco Germano Martins a, Carlos Augusto Silva de Oliveira.Study of full-mold casting process for Al–Si hypoeutectic alloys (2006) 196–201

7- Sudhir Kumar, Pradeep Kumar, H.S. Shan. Effect of evaporative pattern casting process parameters on the surface roughness of Al–7% Si alloy castings

8- Sudhir Kumar∗, Pradeep Kumar, H.S. Shan. Optimization of tensile properties of evaporative pattern casting process through Taguchi's method(2007)

9- M. Khodaia,N. Parvinb . Pressure measurement and some observation in lost foam casting (2007)

10- PHD by Ramin Ajdar)The effect of the mold materials on the solidification microstructure and fluidity of 356 .2001 canada

11- Practices for the repair of automotive sheet aluminum, Copyright 1998 the Aluminum Association, pp 1-23

12- Grain Refinement of Aluminium-Silicon Foundry Alloys. London&

Scandinavian Metallurgical Co. Limited, 1998, pp1-29.

13- Stuart D. McDonald, Eutectic nucleation in Al–Si alloys, 2004, pp4273–4280

14- Kalpakjian, S. and Schmid, S.R. 2001. Manufacturing Engineering and Technology.4th Ed. New Jersey: Prientice Hall.

15- Yao, X., 1994. An Experimental Analysis of Casting Formation in the Expendable Pattern Casting (EPC) Process. M.S. Thesis, Worcester Polytechnic Institute. M.S.Thesis, Worcester Polytechnic Institute.

16- Wang, L., Shivkumar, S. and Apelian, D., 1990. Effects of Polymer Degradation on the Quality of Lost Foam Castings. Transactions of the American Foundrymen's Society 923-933.

17- Shivkumar, S., 1994. Modeling of Temperature Losses in Liquid Metal during Casting Formation in Expendable Pattern Casting Process. Materials Science and Technology, 10 986-992.

18- Hill, M.W., Lawrence, M., Ramsay, C.W. and Askeland, D.R., 1997. Influence of Gating and Other Processing Parameters on Mold Filling in the LFC Process. Transactions of the American Foundrymen's Society, 105: 443-450.117

19- Density and Mechanical Properties of Aluminum Lost Foam Casting by Pressurization during Solidification Bokhyun KANG1), Yongsun KIM1), Kiyoung KIM1)y, Gueserb CHO2), Kyeonghwan CHOE2) and Kyongwhoan LEE2) J. Mater. Sci. Technol., Vol.23 No.6, 2007

20- Investigation of the Performance of an Expandable Polystyrene Injector for Use in the Lost-Foam Casting Process K.F. WALL, S.H. BHAVNANI, R.A. OVERFELT, D.S. SHELDON, and K. WILLIAMS METALLURGICAL AND MATERIALS TRANSACTIONS 2003

21- EPS molecular weight and foam density effects in the lost foam process M. SANDS, S. SHIVKUMAR JOURNAL OF MATERIALS SCIENCE 38 (2003) 2233 – 2239

22- Numerical modeling and experimental verification of mold filling and evolved gas pressure in lost foam casting process Y. LIU, S. I. BAKHTIYAROV, R. A. OVERFELT JOURNAL OF MATERIALS SCIENCE 37 (2002) 2997 – 3003

23- A multi-objective framework for the design of vacuum sealed molding process Pradeep Kumar!, Nanua Singh!,*, Parveen Goel" Robotics and Computer Integrated Manufacturing 15 (1999) 413}422

24- A foam melting model for lost foam casting of aluminum D.A. Caulk International Journal of Heat and Mass Transfer 49 (2006) 2124–2136

25- Characterization of the Refractory Coating Material Used In Vacuum Assisted Evaporative Pattern Casting Process Authors: Sudhir Kumar, Pradeep Kumar, H.S. Shan Journal of Materials Processing Technology 6/2008

26- Compressive behavior of an idealized EPS lightweight concrete: size effects and failure mode K. Miled a, R . Le R oy b, K. Sab a,*, C. Boulay Mechanics of Materials 36 (2004) 1031–1046